THE AMERICAN MINERALOGIST
JOURNAL OF THE MINERALOGICAL SOCIETY OF AMERICA

Vol. 27 OCTOBER, 1942 No. 10

A METHOD FOR THE SUMMATION OF THE FOURIER SERIES USED IN THE X-RAY ANALYSIS OF CRYSTAL STRUCTURES

A. L. PATTERSON,*
Department of Physics, Bryn Mawr College,
AND
GEORGE TUNELL,
Geophysical Laboratory, Carnegie Institution of Washington.

ABSTRACT

This paper describes in detail a method that has proved useful in the summation of one-dimensional Fourier series, and a procedure that enables this method to be applied to the summation of two-dimensional series such as those by which the electron density of a crystal is represented as a function of the coordinates in the projection of the unit cell on a particular plane. The method, like those of Robertson and of Lipson and Beevers, utilizes cardboard strips, each carrying a series of values of a certain trigonometric function, but differs from the other two in that the selection of numbers to be added from a series of strips for a given point of the unit cell is accomplished by one of a set of stencils. Experience has shown that this method is well adapted to the range of F-values (or of $|F|^2$-values) from 0 to 1000.

INTRODUCTION

In recent years there has been a very widespread use of the Fourier series in the analysis of the data obtained by the diffraction of x-rays in crystals. The electron density in a crystal can be represented by a three-dimensional Fourier series in which the coefficients are the structure factors $F(hkl)$, the intensities of the diffraction lines, corrected for certain known trigonometric factors, being proportional to $|F(hkl)|^2$. The projection of the electron density on a plane perpendicular to a zone axis can be represented by a two-dimensional series using only the F's of the reflections in that zone. Various methods[1] which lead to the successful analysis of x-ray data have been devised which depend on the summation of Fourier series. Routine methods for carrying out the summation of such series have therefore become part of the necessary equipment of any laboratory specializing in x-ray analysis.

---

* Work of the senior author supported by the Elizabeth Thompson Science Fund, and the Madge Miller Research Fund of Bryn Mawr College.

[1] For a summary article on such methods see Robertson, J. M.: Reports on Progress in Physics, *Physical Society*, London, **4**, 332 (1938).

The usual methods for summing two- and three-dimensional Fourier series involve splitting these summations into a number of summations of one-dimensional series according to a scheme proposed by Beevers and Lipson.[2] Three numerical methods[3,4,5] have been suggested for the rapid handling of the one-dimensional summations, and it is the purpose of the present paper to describe one of these methods[5] in detail.

The paper is divided into two parts. In the first part, the process for the summation of a one-dimensional Fourier series is discussed and a description of the appliances used by the authors is given. In the second part, an account is given of the routine methods used by us in combining the one-dimensional summations into two-dimensional summations.

Part I. The Summation of One-Dimensional Fourier Series

1. *Simplification of the summation of series by rearrangement of terms*

The method for the summation of one-dimensional series to be described in the present paper is in essential due to L. Hermann[6] who made use of it in the analysis of voice records. The application of the method to Fourier synthesis[5] was made without knowledge of the earlier work. It will be evident to those who have read the original papers, that we have made considerable use of short-cuts suggested by Beevers and Lipson[2,4] and by Robertson.[3] To avoid interruption of the line of argument, acknowledgment of this indebtedness is made here.

In its most general form, a one-dimensional Fourier series may be written

$$f(x) = \sum_{h=-\infty}^{\infty} A(h) \cos 2\pi hx/a + B(h) \sin 2\pi hx/a \tag{1}$$

in which

$$A(h) = A(\bar{h}) \quad \text{and} \quad B(h) = -B(\bar{h}). \tag{1'}$$

Such a series is of course periodic with a period a. We shall usually wish to sum this series at N points which divide the period a into N equal parts. It is thus convenient for our purpose to choose a new coordinate X such that $X = Nx/a$, where X is an integer. We shall call such a coordinate X a coordinate on the base N, and shall use coordinates of this type throughout the remainder of the paper. We then have to sum the two different kinds of series, i.e.

$$C(X) = \sum_{h=-\infty}^{\infty} A(h) \cos 2\pi hX/N \tag{2}$$

---

[2] Beevers, C. A., and Lipson, H.: *Phil. Mag.* (7), **17**, 855 (1934).

[3] Robertson, J. M.: *Phil. Mag.* (7), **21**, 176 (1936).

[4] Lipson, H., and Beevers, C. A.: *Proc. Phys. Soc.*, **48**, 772 (1936).

[5] Patterson, A. L.: *Phil. Mag.* (7), **22**, 753 (1936).

[6] Hermann, L.: *Archiv für die gesammte Physiologie*, **47**, 44 (1890).

and

$$S(X) = \sum_{h=-\infty}^{\infty} B(h) \sin 2\pi hX/N, \tag{3}$$

for $0 \leqq X \leqq N/2$ and to combine the results according to the relations

$$\begin{aligned} f(X) &= C(X) + S(X) \\ f(N-X) &= C(X) - S(X). \end{aligned} \tag{4}$$

We may now reduce the number of terms[7] in the summations (2) and (3) by making use of the two relations

$$\cos 2\pi X(pN \pm h)/N = \cos 2\pi hX/N, \qquad p = 0, \pm 1, \pm 2, \cdots, \tag{5}$$

and

$$\sin 2\pi X(pN \pm h)/N = \pm \sin 2\pi hX/N, \quad p = 0, \pm 1, \pm 2, \cdots.$$

It is thus possible to write (2) and (3) in the forms

$$C(X) = \sum_{h=0}^{N/2} C(h) \cos 2\pi hX/N \tag{6}$$

and

$$S(X) = \sum_{h=0}^{N/2} S(h) \sin 2\pi hX/N \tag{7}$$

respectively, in which

$$\begin{aligned} C(h) &= 2A(h) + 2\sum_{p=1}^{\infty} \{A(pN-h) + A(pN+h)\} \\ S(h) &= 2B(h) - 2\sum_{p=1}^{\infty} \{B(pN-h) - B(pN+h)\} \\ C(0) &= A(0) + 2\sum_{p=1}^{\infty} A(pN) \\ C(N/2) &= 2\sum_{p=0}^{\infty} A(\overline{2p+1}\cdot N/2) \\ S(0) &= S(N/2) = 0.^{8} \end{aligned} \tag{8}$$

If we sum the odd and the even terms of the series (6) and (7) separately, we can still further reduce the number of points over which it will be necessary to compute these series. We note that

$$\begin{aligned} \cos 2\pi h(N/2 - X)/N &= (-1)^h \cos 2\pi hX/N \\ \sin 2\pi h(N/2 - X)/N &= (-1)^{h+1} \sin 2\pi hX/N \end{aligned} \tag{9}$$

---

[7] If the indices of the planes for which x-ray intensities are available are all less than $N/2$, and this is the common case, the full analysis of this paragraph is unnecessary. In this case the coefficients of the series (6) and (7) are given by $C(h) = 2A(h)$; $S(h) = 2B(h)$; $C(0) = A(0)$; and $S(0) = 0$ instead of the more complicated expressions (8).

[8] This last result follows from the fact that

$$\sin 2\pi \left(\frac{pN}{2}\,\frac{X}{N}\right) = \sin \pi pX = 0$$

so that the terms whose coefficients are $B(pN/2)$ make no contribution to the sum (3 and, if N is an even number,

$$\begin{aligned} C(X) &= C_e(X) + {}_o(CX) \\ C(N/2 - X) &= C_e(X) - C_o(X) \\ S(X) &= S_e(X) + S_o(X) \\ S(N/2 - X) &= -S_e(X) + S_o(X) \end{aligned} \tag{10}$$

provided that C_e and S_e are the partial sums of the even terms and C_o and S_o are the partial sums of the odd terms of the series $C(X)$ and $S(X)$ respectively.

2. *A stencil method for the summation of sine and cosine series*

In the last section we have seen that the summation of the Fourier series (1) can be reduced to a number of summations of one of two types, i.e.

$$\sum_{h=0}^{N/2} C(h) \cos 2\pi hX/N \qquad (11a) \qquad \text{or} \qquad \sum_{h=1}^{N/2} S(h) \sin 2\pi hX/N. \qquad (11b)$$

In these summations we shall be concerned with X values in the range between zero and $N/4$ and either even or odd values of h in the range including zero and $N/2$. If we could have available all possible products of the type $D \cos 2\pi hX/N$ or $D \sin 2\pi hX/N$ in which D were any number which we might meet as a C or an S coefficient, then the summations (11) would be reduced to mere additions. If we notice that

$$\sin 2\pi(N/4 - hX)/N = \cos 2\pi hX/N$$

and that $(N/4 - hX)$ and hX are both integers if N is divisible by 4 we, see that all possible *numerical* values of $D \cos 2\pi hX/N$ or $D \sin 2\pi hX/N$ will be listed if we list the values

$$D \cos 2\pi s/N \quad (s = 0, 1, 2, \cdots, N/4)$$

for all values of D which we may meet as coefficients $C(h)$ or $S(h)$, where s is the number of the position in the series reading from left to right. Such listings are conveniently arranged on cardboard strips. Typical strips are shown in Fig. 1. The strips corresponding to positive D values are of white card; those corresponding to negative D values are of card of a different color.

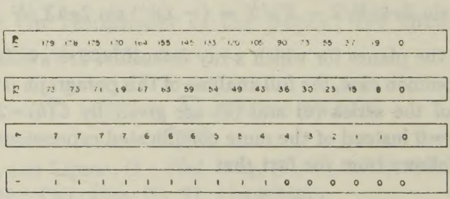

FIG. 1. Typical strips for $N=60$. The numbers shown are $D \cos (s6°)$, where s gives the position of the number on the strip ($s=0, 1, \cdots, 15$). The D-values shown are 179, 73, 7, and 1, respectively.

In forming the sums C_e and C_o, a strip is selected for each value of $C(h)$. There will be, at the most, $(N/2+1)$ such strips, which are then arranged in order of their h values in a grooved rack (Figs. 2*a* and 2*b*).

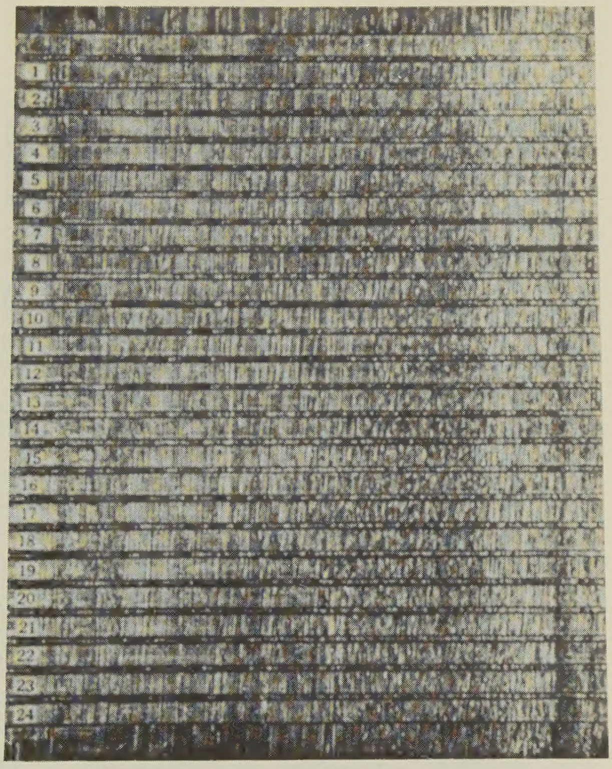

FIG. 2a. Rack for $N=48$ to handle h values 0 to 25.

These strips in their rack (Figs. 3*a* and 3*c*) then form a table which contains all the *numerical* values which will be needed in the computation of the sums C_e and C_o, that is in the computation of the series $C(X)$ of equation (2). It only remains to devise some means of selecting the values needed in making the summation for a particular point. This is done by means of a set of stencils. There is a C_e and a C_o stencil for each value of X. In these stencils the openings are arranged to select the correct numerical value for a given h. One such stencil is shown in place in each of the racks in Fig. 3*b*. The holes which select the positive values are unmarked, while those corresponding to negative values are ringed with appropriate paint. When the number seen through a ringed hole is on a colored card the number is to be taken with a positive sign, the negative property of the ringed hole offsetting the negative property of the colored strip.

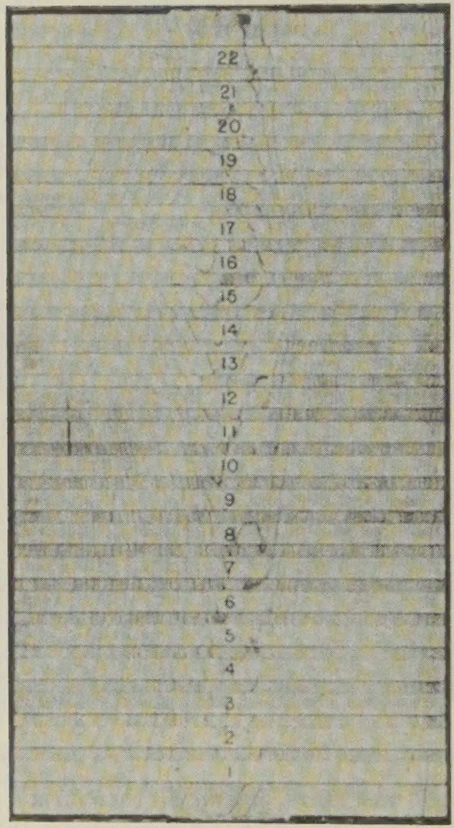

FIG. 2b. Rack for $N=60$ to handle h values 1 to 22. (Note. The rack for $N=60$ would have a greater range of utility if additional slots for $h=23$ to 30 inclusive were present, although no case has yet been encountered where these additional slots were needed. A slot for $h=0$ would add slightly to the convenience of use.)

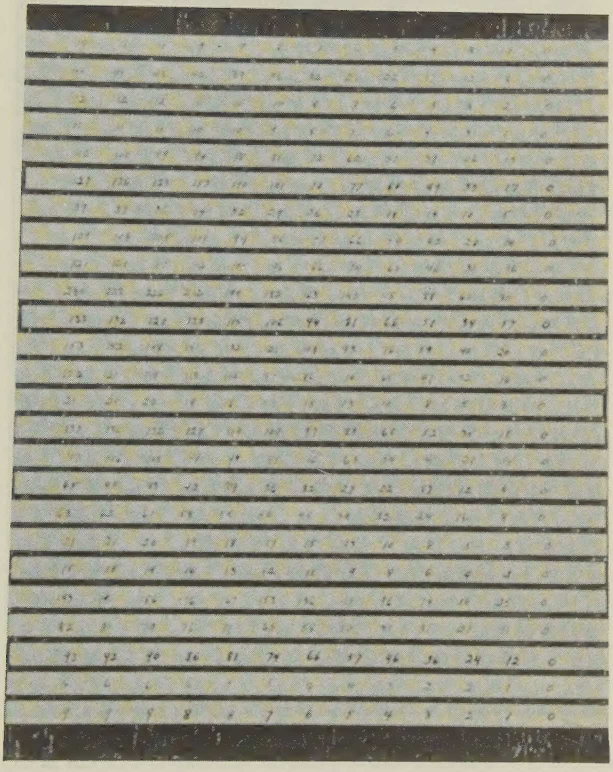

FIG. 3a. Rack for $N=48$ with strips in place.

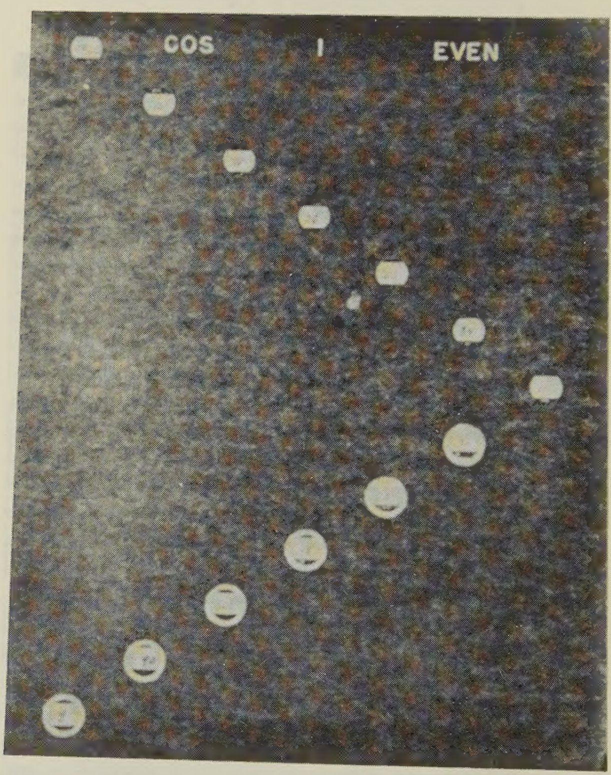

Fig. 3b. Rack for $N=48$ with stencil in place for summation $C(h) \cos 2\pi hX/N$ for $X=1$, even indices.

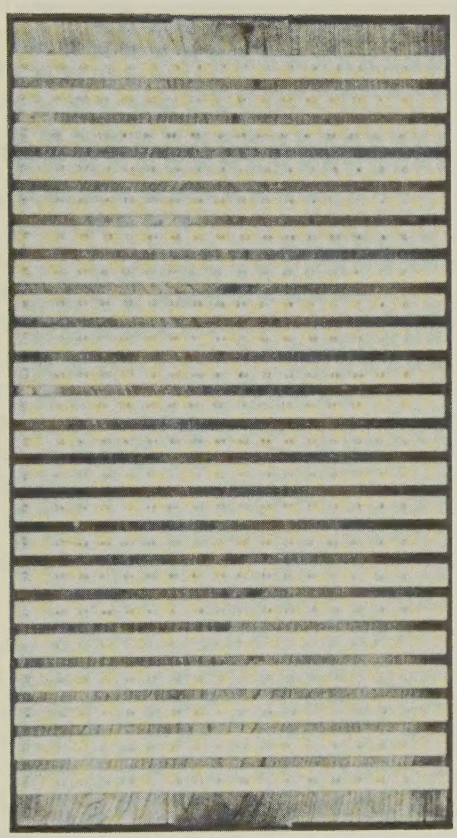

FIG. 3c. Rack for $N=60$ with strips in place.

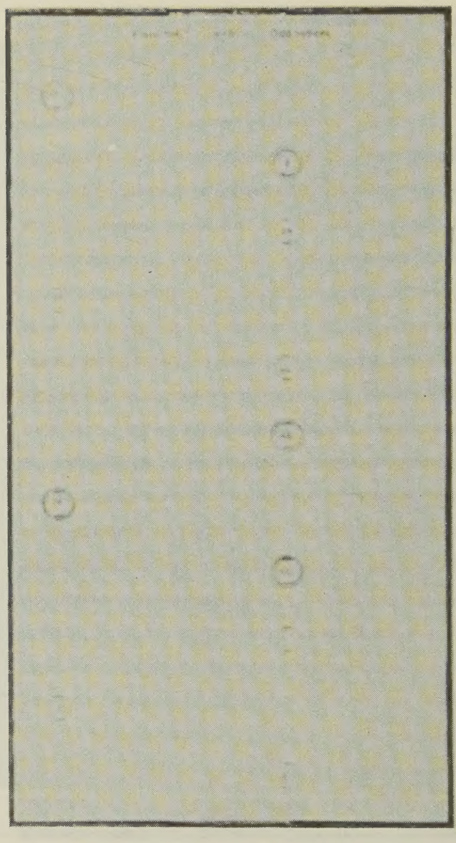

FIG. 3d. Rack for $N=60$ with stencil in place for summation $S(h)$ sin $2\pi hX/N$ for $X=5$, odd indices.

In a similar manner strips can be selected and racked so as to build up a table containing all the numerical values which will be needed in the computation of the sums S_e and S_o. The same set of strips can be used for sine and cosine summations, but in the case of the sine summations the numbers on the strips are taken as representing $D \sin 2\pi(N/4-s)/N$, $(s=0, 1, \cdot \quad \cdot, N/4)$, where s as before is the number of the position on the strip reading from left to right. Another set of stencils can then be arranged to select from this table the values necessary for the summations S_e and S_o for each value of X (Fig. 3*d*).

3. *Layout for stencils*

In describing the layout scheme for a set of stencils, we shall discuss in considerable detail the case of $N=20$. For this small value of N we can illustrate the full set of stencils and describe the process of laying them out. We shall then give the tables that are needed to make the layouts necessary for the more useful values $N=48$ and $N=60$. After study of these tables the reader should be in a position to set up such tables for himself for any other values of N that may be needed.

In making a cosine summation one strip is chosen for each $C(h)$ value and placed in the hth position in the rack. For a given X and a given h we shall need to select the value

$$C(h) \cos 2\pi hX/N$$

from among the values

$$C(h) \cos 2\pi s/N$$

carried on the strip in the hth position on the rack. A table must therefore be constructed of the s values corresponding to given values of h and X for a specified N. Such a table is given below for cosine summations for $N=20$, $X=0, 1, \cdots, 5$ and $h=0, 1, \cdots, 10$. The s values for a given h appear in a vertical column, while those for a given X appear in a horizontal row. The C_e and C_o stencils for $X=0$ thus have all 0 values of s and therefore select values of $C(h) \cos 2\pi s/N$ corresponding to $\cos 2\pi s/N=1$. The correct arrangement of holes for this stencil is shown in Fig. 4 in the stencil labelled[9] "Cos, $X=0$, h even" which selects the values $C(h)$ for all h even. Similarly the stencil "Cos, $X=0$, h odd" selects the values $C(h)$ for all h odd. The "Cos, $X=1$, h even" stencil selects the values $C(0)$, $C(2) \cos 4\pi/20$, $C(4) \cos 8\pi/20$, $-C(6) \cos 8\pi/20$, $-C(8) \cos 4\pi/20$, $-C(10)$. These are then added to give the partial sum $C_e(X)$ obtained by adding the even terms of the series (6). In Figs. 3*b* and

---

[9] In labelling stencils, one of us (P.) has used the abbreviated notation shown on the stencil of Fig. 3*b* for $N=48$; the other (T.) has used the more detailed label shown on the $N=60$ stencil of Fig. 3*d*.

TABLE 1. TABLE OF VALUES OF s AS FUNCTION OF h AND X FOR COSINE STENCILS ($N=20$). A LINE UNDER THE s VALUE INDICATES A NEGATIVE VALUE FOR $D \cos 2\pi s/N$

X \ h	0	1	2	3	4	5	6	7	8	9	10
0	0	0	0	0	0	0	0	0	0	0	0
1	0	1	2	3	4	5	$\underline{4}$	$\underline{3}$	$\underline{2}$	$\underline{1}$	$\underline{0}$
2	0	2	4	$\underline{4}$	$\underline{2}$	$\underline{0}$	$\underline{2}$	$\underline{4}$	4	2	0
3	0	3	$\underline{4}$	$\underline{1}$	$\underline{2}$	5	2	1	4	$\underline{3}$	$\underline{0}$
4	0	4	$\underline{2}$	$\underline{2}$	4	0	4	$\underline{2}$	$\underline{2}$	4	0
5	0	5	$\underline{0}$	5	0	5	$\underline{0}$	5	0	5	$\underline{0}$

3d stencils are shown in place on the racks for $N=48$ and $N=60$. The reader can easily assure himself that the other cosine stencils will select the appropriate values to form the partial sums of the odd terms and the even terms of the series (6) for various values of X.

To sum the series (7) we must place in the rack the strips

$$S(h) \cos 2\pi s/N$$

and plan a set of stencils to select from among them the values which correspond to the quantities

$$S(h) \sin 2\pi hX/N$$

needed in forming the partial sums of the odd and even terms of the series (7). The appropriate s values are shown in Table 2.

TABLE 2. TABLE OF VALUES OF s AS FUNCTION OF h AND X FOR SINE STENCILS ($N=20$)

X \ h	0	1	2	3	4	5	6	7	8	9	10
0	5	5	5	5	5	5	5	5	5	5	5
1	5	4	3	2	1	0	1	2	3	4	5
2	5	3	1	1	3	5	$\underline{3}$	$\underline{1}$	$\underline{1}$	$\underline{3}$	5
3	5	2	1	4	$\underline{3}$	$\underline{0}$	$\underline{3}$	4	1	2	5
4	5	1	3	$\underline{3}$	$\underline{1}$	5	1	3	$\underline{3}$	$\underline{1}$	5
5	5	0	5	$\underline{0}$	5	0	5	$\underline{0}$	5	0	5

The sine stencils constructed on this scheme are also illustrated in Fig. 3. It is easily seen that the backs of the cosine stencils can be used for the sine stencils.

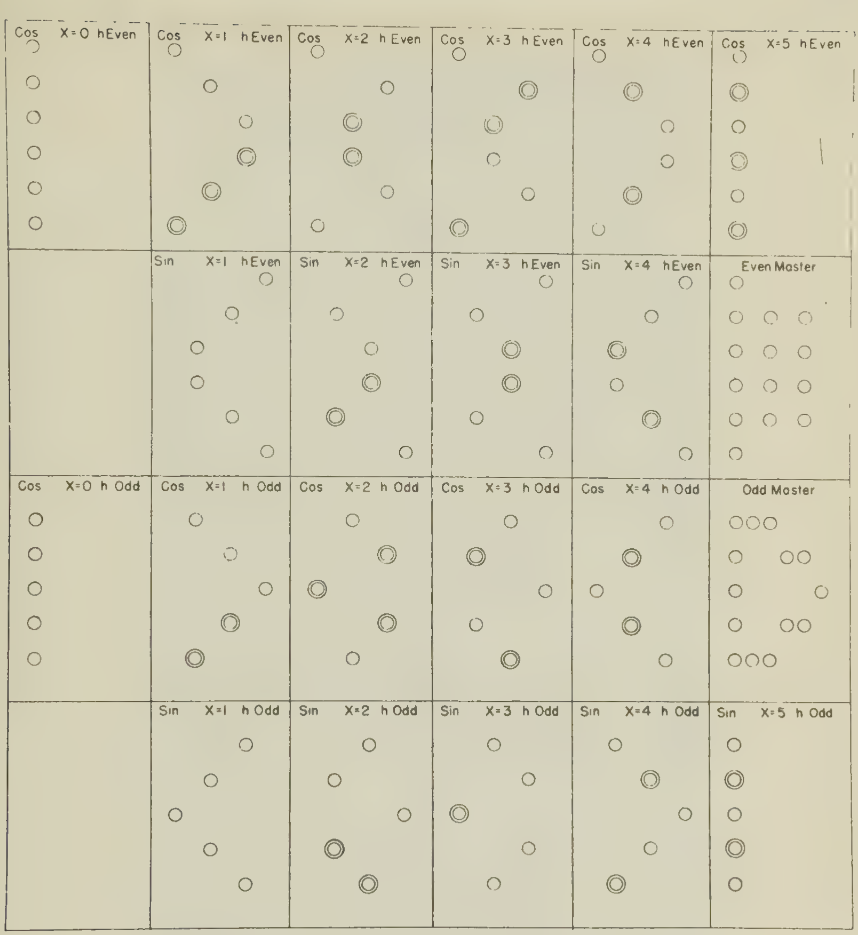

FIG. 4. Layout of stencils for $N=20$. The ringed holes correspond to negative values. The same cards can be used for the sine and the cosine stencils, one side of each card serving for the cosine summation and the other side for the sine summation.

In Tables 3–6 the s values are given for the cosine and sine stencils for $N=48$ and $N=60$. Both these values of N have been found satisfactory in the laboratories of the writers and elsewhere for the summation of the Fourier series that arise in x-ray analysis. If the reader wishes to use any other value of N, he will find it easy to construct corresponding tables provided that N is divisible by 4.

TABLE 3. TABLE OF VALUES OF s AS FUNCTION OF h AND X FOR COSINE STENCILS ($N=48$)

h X	0	1	2	3	4	5	6	7	8	9	10	11	12	13	14	15	16	17	18	19	20	21	22	23	24
0	0	0	0	0	0	0	0	0	0	0	0	0	0	0	0	0	0	0	0	0	0	0	0	0	0
1	0	1	2	3	4	5	6	7	8	9	10	11	12	$\underline{11}$	$\underline{10}$	$\underline{9}$	$\underline{8}$	$\underline{7}$	$\underline{6}$	$\underline{5}$	$\underline{4}$	$\underline{3}$	$\underline{2}$	$\underline{1}$	$\underline{0}$
2	0	2	4	6	8	10	12	$\underline{10}$	$\underline{8}$	$\underline{6}$	$\underline{4}$	$\underline{2}$	$\underline{0}$	$\underline{2}$	$\underline{4}$	$\underline{6}$	$\underline{8}$	$\underline{10}$	12	10	8	6	4	2	0
3	0	3	6	9	12	$\underline{9}$	$\underline{6}$	$\underline{3}$	$\underline{0}$	$\underline{3}$	$\underline{6}$	$\underline{9}$	12	9	6	3	0	3	6	9	12	$\underline{9}$	$\underline{6}$	$\underline{3}$	$\underline{0}$
4	0	4	8	12	$\underline{8}$	$\underline{4}$	$\underline{0}$	$\underline{4}$	$\underline{8}$	12	8	4	0	4	8	12	$\underline{8}$	$\underline{4}$	$\underline{0}$	$\underline{4}$	$\underline{8}$	12	8	4	0
5	0	5	10	$\underline{9}$	$\underline{4}$	$\underline{1}$	$\underline{6}$	$\underline{11}$	8	3	2	7	12	$\underline{7}$	$\underline{2}$	$\underline{3}$	$\underline{8}$	11	6	1	4	9	$\underline{10}$	$\underline{5}$	$\underline{0}$
6	0	6	12	$\underline{6}$	$\underline{0}$	$\underline{6}$	12	6	0	6	12	$\underline{6}$	$\underline{0}$	$\underline{6}$	12	6	0	6	12	$\underline{6}$	$\underline{0}$	$\underline{6}$	12	6	0
7	0	7	$\underline{10}$	$\underline{3}$	$\underline{4}$	$\underline{11}$	6	1	8	$\underline{9}$	$\underline{2}$	$\underline{5}$	12	5	2	9	$\underline{8}$	$\underline{1}$	$\underline{6}$	11	4	3	10	$\underline{7}$	$\underline{0}$
8	0	8	$\underline{8}$	$\underline{0}$	$\underline{8}$	8	0	8	$\underline{8}$	$\underline{0}$	$\underline{8}$	8	0	8	$\underline{8}$	$\underline{0}$	$\underline{8}$	8	0	8	$\underline{8}$	$\underline{0}$	$\underline{8}$	8	0
9	0	9	$\underline{6}$	$\underline{3}$	12	3	6	$\underline{9}$	$\underline{0}$	$\underline{9}$	6	3	12	$\underline{3}$	$\underline{6}$	9	0	9	$\underline{6}$	$\underline{3}$	12	3	6	$\underline{9}$	$\underline{0}$
10	0	10	$\underline{4}$	$\underline{6}$	8	2	12	$\underline{2}$	$\underline{8}$	6	4	$\underline{10}$	$\underline{0}$	$\underline{10}$	4	6	$\underline{8}$	$\underline{2}$	12	2	8	$\underline{6}$	$\underline{4}$	10	0
11	0	11	$\underline{2}$	$\underline{9}$	4	7	$\underline{6}$	$\underline{5}$	8	3	$\underline{10}$	$\underline{1}$	12	1	10	$\underline{3}$	$\underline{8}$	5	6	$\underline{7}$	$\underline{4}$	9	2	$\underline{11}$	$\underline{0}$
12	0	12	$\underline{0}$	12	0	12	$\underline{0}$	12	0	12	$\underline{0}$	12	0	12	$\underline{0}$	12	0	12	$\underline{0}$	12	0	12	$\underline{0}$	12	0

TABLE 4. TABLE OF VALUES OF s AS FUNCTION OF h AND X FOR SINE STENCILS ($N=48$)

X \ h	0	1	2	3	4	5	6	7	8	9	10	11	12	13	14	15	16	17	18	19	20	21	22	23	24
0	12	12	12	12	12	12	12	12	12	12	12	12	12	12	12	12	12	12	12	12	12	12	12	12	12
1	12	11	10	9	8	7	6	5	4	3	2	1	0	1	2	3	4	5	6	7	8	9	10	11	12
2	12	10	8	6	4	2	0	2	4	6	8	10	12	$\underline{10}$	$\underline{8}$	$\underline{6}$	$\underline{4}$	$\underline{2}$	$\underline{0}$	$\underline{2}$	$\underline{4}$	$\underline{6}$	$\underline{8}$	$\underline{10}$	12
3	12	9	6	3	0	3	6	9	12	$\underline{9}$	$\underline{6}$	$\underline{3}$	$\underline{0}$	$\underline{3}$	$\underline{6}$	$\underline{9}$	12	9	6	3	0	3	6	9	12
4	12	8	4	0	4	8	12	$\underline{8}$	$\underline{4}$	$\underline{0}$	$\underline{4}$	$\underline{8}$	12	8	4	0	4	8	12	$\underline{8}$	$\underline{4}$	$\underline{0}$	$\underline{4}$	$\underline{8}$	12
5	12	7	2	3	8	$\underline{11}$	$\underline{6}$	$\underline{1}$	$\underline{4}$	$\underline{9}$	10	5	0	5	10	$\underline{9}$	$\underline{4}$	$\underline{1}$	$\underline{6}$	$\underline{11}$	8	3	2	7	12
6	12	6	0	6	12	$\underline{6}$	$\underline{0}$	$\underline{6}$	12	6	0	6	12	$\underline{6}$	$\underline{0}$	$\underline{6}$	12	6	0	6	12	$\underline{6}$	$\underline{0}$	$\underline{6}$	12
7	12	5	2	9	$\underline{8}$	$\underline{1}$	$\underline{6}$	11	4	3	10	$\underline{7}$	$\underline{0}$	$\underline{7}$	10	3	4	11	$\underline{6}$	$\underline{1}$	$\underline{8}$	9	2	5	12
8	12	4	4	12	$\underline{4}$	$\underline{4}$	12	4	4	12	$\underline{4}$	$\underline{4}$	12	4	4	12	$\underline{4}$	$\underline{4}$	12	4	4	12	$\underline{4}$	$\underline{4}$	12
9	12	3	6	$\underline{9}$	$\underline{0}$	$\underline{9}$	6	3	12	$\underline{3}$	$\underline{6}$	9	0	9	$\underline{6}$	$\underline{3}$	12	3	6	$\underline{9}$	$\underline{0}$	$\underline{9}$	6	3	12
10	12	2	8	$\underline{6}$	$\underline{4}$	10	0	10	$\underline{4}$	$\underline{6}$	8	2	12	$\underline{2}$	$\underline{8}$	6	4	$\underline{10}$	$\underline{0}$	$\underline{10}$	4	6	$\underline{8}$	$\underline{2}$	12
11	12	1	10	$\underline{3}$	$\underline{8}$	5	6	$\underline{7}$	$\underline{4}$	9	2	$\underline{11}$	$\underline{0}$	$\underline{11}$	2	9	$\underline{4}$	$\underline{7}$	6	5	$\underline{8}$	$\underline{3}$	10	1	12
12	12	0	12	$\underline{0}$	12	0	12	$\underline{0}$	12	0	12	$\underline{0}$	12	0	12	$\underline{0}$	12	0	12	$\underline{0}$	12	0	12	$\underline{0}$	12

TABLE 5. TABLE OF VALUES OF s AS FUNCTION OF h AND X FOR COSINE STENCILS ($N=60$)

$X \backslash h$	0	1	2	3	4	5	6	7	8	9	10	11	12	13	14	15	16	17	18	19	20	21	22	23	24	25	26	27	28	29	30
0	0	0	0	0	0	0	0	0	0	0	0	0	0	0	0	0	0	0	0	0	0	0	0	0	0	0	0	0	0	0	0
1	0	1	2	3	4	5	6	7	8	9	10	11	12	13	14	15	$\underline{14}$	$\underline{13}$	$\underline{12}$	$\underline{11}$	$\underline{10}$	$\underline{9}$	$\underline{8}$	$\underline{7}$	$\underline{6}$	$\underline{5}$	$\underline{4}$	$\underline{3}$	$\underline{2}$	$\underline{1}$	$\underline{0}$
2	0	2	4	6	8	10	12	14	$\underline{14}$	$\underline{12}$	$\underline{10}$	$\underline{8}$	$\underline{6}$	$\underline{4}$	$\underline{2}$	$\underline{0}$	$\underline{2}$	$\underline{4}$	$\underline{6}$	$\underline{8}$	$\underline{10}$	$\underline{12}$	$\underline{14}$	14	12	10	8	6	4	2	0
3	0	3	6	9	12	15	$\underline{12}$	$\underline{9}$	$\underline{6}$	$\underline{3}$	$\underline{0}$	$\underline{3}$	$\underline{6}$	$\underline{9}$	$\underline{12}$	15	12	9	6	3	0	3	6	9	12	15	$\underline{12}$	$\underline{9}$	$\underline{6}$	$\underline{3}$	$\underline{0}$
4	0	4	8	12	$\underline{14}$	$\underline{10}$	$\underline{6}$	$\underline{2}$	$\underline{2}$	$\underline{6}$	$\underline{10}$	$\underline{14}$	12	8	4	0	4	8	12	$\underline{14}$	$\underline{10}$	$\underline{6}$	$\underline{2}$	$\underline{2}$	$\underline{6}$	$\underline{10}$	$\underline{14}$	12	8	4	0
5	0	5	10	15	$\underline{10}$	$\underline{5}$	$\underline{0}$	$\underline{5}$	$\underline{10}$	15	10	5	0	5	10	15	$\underline{10}$	$\underline{5}$	$\underline{0}$	$\underline{5}$	$\underline{10}$	15	10	5	0	5	10	15	$\underline{10}$	$\underline{5}$	$\underline{0}$
6	0	6	12	$\underline{12}$	$\underline{6}$	$\underline{0}$	$\underline{6}$	$\underline{12}$	12	6	0	6	12	$\underline{12}$	$\underline{6}$	$\underline{0}$	$\underline{6}$	$\underline{12}$	12	6	0	6	12	$\underline{12}$	$\underline{6}$	$\underline{0}$	$\underline{6}$	$\underline{12}$	12	6	0
7	0	7	14	$\underline{9}$	$\underline{2}$	$\underline{5}$	$\underline{12}$	11	4	3	10	$\underline{13}$	$\underline{6}$	$\underline{1}$	$\underline{8}$	15	8	1	6	13	$\underline{10}$	$\underline{3}$	$\underline{4}$	$\underline{11}$	12	5	2	9	$\underline{14}$	$\underline{7}$	$\underline{0}$
8	0	8	$\underline{14}$	$\underline{6}$	$\underline{2}$	$\underline{10}$	12	4	4	12	$\underline{10}$	$\underline{2}$	$\underline{6}$	$\underline{14}$	8	0	8	$\underline{14}$	$\underline{6}$	$\underline{2}$	$\underline{10}$	12	4	4	12	$\underline{10}$	$\underline{2}$	$\underline{6}$	$\underline{14}$	8	0
9	0	9	$\underline{12}$	$\underline{3}$	$\underline{6}$	15	6	3	12	$\underline{9}$	$\underline{0}$	$\underline{9}$	12	3	6	15	$\underline{6}$	$\underline{3}$	$\underline{12}$	9	0	9	$\underline{12}$	$\underline{3}$	$\underline{6}$	15	6	3	12	$\underline{9}$	$\underline{0}$
10	0	10	$\underline{10}$	$\underline{0}$	$\underline{10}$	10	0	10	$\underline{10}$	$\underline{0}$	$\underline{10}$	10	0	10	$\underline{10}$	$\underline{0}$	$\underline{10}$	10	0	10	$\underline{10}$	$\underline{0}$	$\underline{10}$	10	0	10	$\underline{10}$	$\underline{0}$	$\underline{10}$	10	0
11	0	11	$\underline{8}$	$\underline{3}$	$\underline{14}$	5	6	$\underline{13}$	$\underline{2}$	$\underline{9}$	10	1	12	$\underline{7}$	$\underline{4}$	15	4	7	$\underline{12}$	$\underline{1}$	$\underline{10}$	9	2	13	$\underline{6}$	$\underline{5}$	14	3	8	$\underline{11}$	$\underline{0}$
12	0	12	$\underline{6}$	$\underline{6}$	12	0	12	$\underline{6}$	$\underline{6}$	12	0	12	$\underline{6}$	$\underline{6}$	12	0	12	$\underline{6}$	$\underline{6}$	12	0	12	$\underline{6}$	$\underline{6}$	12	0	12	$\underline{6}$	$\underline{6}$	12	0
13	0	13	$\underline{4}$	$\underline{9}$	8	5	$\underline{12}$	$\underline{1}$	$\underline{14}$	3	10	$\underline{7}$	$\underline{6}$	11	2	15	$\underline{2}$	$\underline{11}$	6	7	$\underline{10}$	$\underline{3}$	14	1	12	$\underline{5}$	$\underline{8}$	9	4	$\underline{13}$	$\underline{0}$
14	0	14	$\underline{2}$	$\underline{12}$	4	10	$\underline{6}$	$\underline{8}$	8	6	$\underline{10}$	$\underline{4}$	12	2	$\underline{14}$	$\underline{0}$	$\underline{14}$	2	12	$\underline{4}$	$\underline{10}$	6	8	$\underline{8}$	$\underline{6}$	10	4	$\underline{12}$	$\underline{2}$	14	0
15	0	15	$\underline{0}$	15	0	15	$\underline{0}$	15	0	15	$\underline{0}$	15	0	15	$\underline{0}$	15	0	15	$\underline{0}$	15	0	15	$\underline{0}$	15	0	15	$\underline{0}$	15	0	15	$\underline{0}$

Table 6. Table of Values of s as Functions of h and X for Sine Stencils ($N=60$)

X \ h	0	1	2	3	4	5	6	7	8	9	10	11	12	13	14	15	16	17	18	19	20	21	22	23	24	25	26	27	28	29	30
0	15	15	15	15	15	15	15	15	15	15	15	15	15	15	15	15	15	15	15	15	15	15	15	15	15	15	15	15	15	15	15
1	15	14	13	12	11	10	9	8	7	6	5	4	3	2	1	0	1	2	3	4	5	6	7	8	9	10	11	12	13	14	15
2	15	13	11	9	7	5	3	1	1	3	5	7	9	11	13	15	$\underline{13}$	$\underline{11}$	$\underline{9}$	$\underline{7}$	$\underline{5}$	$\underline{3}$	$\underline{1}$	$\underline{1}$	$\underline{3}$	$\underline{5}$	$\underline{7}$	$\underline{9}$	$\underline{11}$	$\underline{13}$	15
3	15	12	9	6	3	0	3	6	9	12	15	$\underline{12}$	$\underline{9}$	$\underline{6}$	$\underline{3}$	$\underline{0}$	$\underline{3}$	$\underline{6}$	$\underline{9}$	$\underline{12}$	15	12	9	6	3	0	3	6	9	12	15
4	15	11	7	3	1	5	9	13	$\underline{13}$	$\underline{9}$	$\underline{5}$	$\underline{1}$	$\underline{3}$	$\underline{7}$	$\underline{11}$	15	11	7	3	1	5	9	13	$\underline{13}$	$\underline{9}$	$\underline{5}$	$\underline{1}$	$\underline{3}$	$\underline{7}$	$\underline{11}$	15
5	15	10	5	0	5	10	15	$\underline{10}$	$\underline{5}$	$\underline{0}$	$\underline{5}$	$\underline{10}$	15	10	5	0	5	10	15	$\underline{10}$	$\underline{5}$	$\underline{0}$	$\underline{5}$	$\underline{10}$	15	10	5	0	5	10	15
6	15	9	3	3	9	15	$\underline{9}$	$\underline{3}$	$\underline{3}$	$\underline{9}$	15	9	3	3	9	15	$\underline{9}$	$\underline{3}$	$\underline{3}$	$\underline{9}$	15	9	3	3	9	15	$\underline{9}$	$\underline{3}$	$\underline{3}$	$\underline{9}$	15
7	15	8	1	6	13	$\underline{10}$	$\underline{3}$	$\underline{4}$	$\underline{11}$	12	5	2	9	$\underline{14}$	$\underline{7}$	$\underline{0}$	$\underline{7}$	$\underline{14}$	9	2	5	12	$\underline{11}$	$\underline{4}$	$\underline{3}$	$\underline{10}$	13	6	1	8	15
8	15	7	1	9	$\underline{13}$	$\underline{5}$	$\underline{3}$	$\underline{11}$	11	3	5	13	$\underline{9}$	$\underline{1}$	$\underline{7}$	15	7	1	9	$\underline{13}$	$\underline{5}$	$\underline{3}$	$\underline{11}$	11	3	5	13	$\underline{9}$	$\underline{1}$	$\underline{7}$	15
9	15	6	3	12	$\underline{9}$	$\underline{0}$	$\underline{9}$	12	3	6	15	$\underline{6}$	$\underline{3}$	$\underline{12}$	9	0	9	$\underline{12}$	$\underline{3}$	$\underline{6}$	15	6	3	12	$\underline{9}$	$\underline{0}$	$\underline{9}$	12	3	6	15
10	15	5	5	15	$\underline{5}$	$\underline{5}$	15	5	5	15	$\underline{5}$	$\underline{5}$	15	5	5	15	$\underline{5}$	$\underline{5}$	15	5	5	15	$\underline{5}$	$\underline{5}$	15	5	5	15	$\underline{5}$	$\underline{5}$	15
11	15	4	7	$\underline{12}$	$\underline{1}$	$\underline{10}$	9	2	13	$\underline{6}$	$\underline{5}$	14	3	8	$\underline{11}$	$\underline{0}$	$\underline{11}$	8	3	14	$\underline{5}$	$\underline{6}$	13	2	9	$\underline{10}$	$\underline{1}$	$\underline{12}$	7	4	15
12	15	3	9	$\underline{9}$	$\underline{3}$	15	3	9	$\underline{9}$	$\underline{3}$	15	3	9	$\underline{9}$	$\underline{3}$	15	3	9	$\underline{9}$	$\underline{3}$	15	3	9	$\underline{9}$	$\underline{3}$	15	3	9	$\underline{9}$	$\underline{3}$	15
13	15	2	11	$\underline{6}$	$\underline{7}$	10	3	$\underline{14}$	$\underline{1}$	$\underline{12}$	5	8	$\underline{9}$	$\underline{4}$	13	0	13	$\underline{4}$	$\underline{9}$	8	5	$\underline{12}$	$\underline{1}$	$\underline{14}$	3	10	$\underline{7}$	$\underline{6}$	11	2	15
14	15	1	13	$\underline{3}$	$\underline{11}$	5	9	$\underline{7}$	$\underline{7}$	9	5	$\underline{11}$	$\underline{3}$	13	1	15	$\underline{1}$	$\underline{13}$	3	11	$\underline{5}$	$\underline{9}$	7	7	$\underline{9}$	$\underline{5}$	11	3	$\underline{13}$	$\underline{1}$	15
15	15	0	15	$\underline{0}$	15	0	15	$\underline{0}$	15	0	15	$\underline{0}$	15	0	15	$\underline{0}$	15	0	15	$\underline{0}$	15	0	15	$\underline{0}$	15	0	15	$\underline{0}$	15	0	15

4. *The construction of strips, racks, and stencils*

The strips upon which the values of $D \cos 2\pi s/N$ are tabulated can be prepared in any width suitable for the type of lettering used. One of us (P.) has used strips of width $\frac{5}{16}''$. The numbers were entered freehand, using a guide to insure their correct location with respect to the stencil openings. For $N=48$ a length of $8\frac{1}{2}''$ proved appropriate. In another case (T.) strips of width $\frac{1}{2}''$ were used and a length of $9\frac{1}{2}''$ proved appropriate for $N=60$. A Leroy lettering guide (#3240 120CL) was used in entering the numbers on the strips in this case. In both cases, white card was used for the positive values, while another color (green or blue) was chosen for the negative values. The strips may be cut to appropriate size in a printer's guillotine or on a sheet metal cutter.

The rack for the strips can be cut out of hardwood or aluminum with the aid of a milling cutter whose width is slightly greater than that of the strips. The depth of the grooves should be equal to the thickness of the strips, so that the filled board presents a flat surface on which the stencils may rest. Brass strips around the edge of the board serve to locate the stencils accurately with respect to the rack. The details of the construction of the board can be readily seen in Figs. 2*a* and 2*b*.

The stencils can be cut from pressboard or other similar material. The positions of the holes are laid out on master stencils (cf. Fig. 3) in accordance with the scheme adopted in laying out the rack and the strips. The holes in the stencils may then be cut out with a hand punch using the master stencil as a guide, or a punch press may be used. The writers have made use of a simple punch mounted in a drill press. The male punch was mounted in the chuck of a drill press, while the female punch was located in a flat board clamped to the table of the press. If pressboard is used for the stencils, the identification marks can be lettered on them in Duco white with use of a Leroy lettering pen with the cleaner removed.

The strips must be stored in such a manner as to make them readily available. The container used by one of us (T.) is illustrated in Fig. 5; it has a separate hole for strips of each D value. The positive and negative strips of the same D value are filed in the same hole with the negative strips placed in the rear. The method is only limited in extent of D values by the convenience of filing the strips. The storage container shown has 208 holes for D values from 0 to 207 inclusive. A convenient container could be made on the same design to accommodate strips with D values 0 to 1000 inclusive.

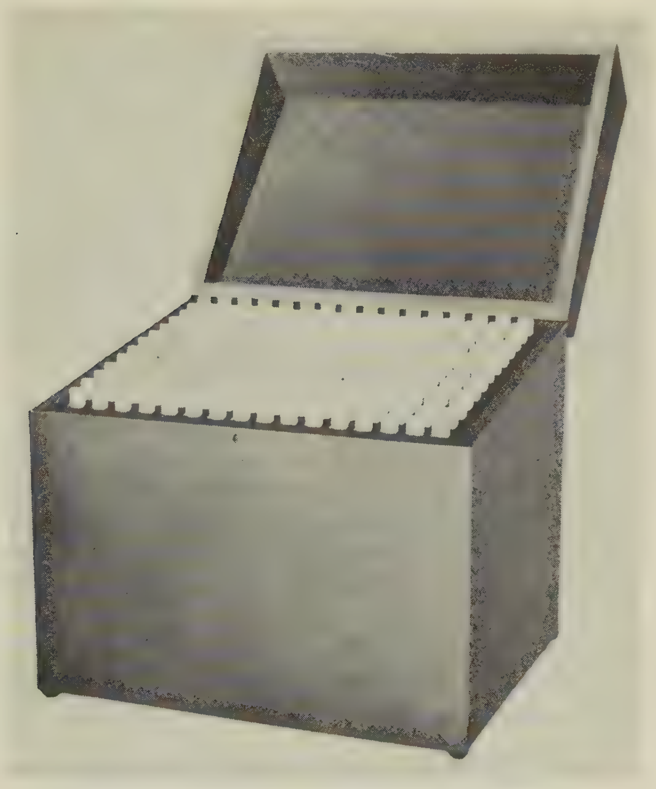

FIG. 5. Container for strips for $N=60$, with places for strips for D-values 0 to 207. The positive and negative strips of the same D-value are filed in the same hole.

PART II. METHODS FOR TWO-DIMENSIONAL SUMMATIONS

5. *The summation of two-dimensional series*

The two-dimensional series which appear in crystal analysis are of the form[10]

$$f(X'Y') = \sum_{h=-\infty}^{\infty} \sum_{k=-\infty}^{\infty} \{A(hk) \cos 2\pi(hX' + kY') + B(hk) \sin 2\pi(hX' + kY')\} \qquad (12)$$

where

$$X' = \frac{X}{N}, \qquad X = 0, \pm 1, \pm 2, \cdots, \pm N,$$

---

[10] Bragg, W. L.: *Proc. Roy. Soc.*, **A123,** 537 (1929); Robertson, J. M.: *Reports on Progress in Physics,* **4,** 332 (1938).

Cf. especially equation II*a*, p. 3, Lonsdale, K.: Simplified Structure Factor and Electron Density Formulae for the 230 Space Groups of Mathematical Crystallography, Bell & Sons, London (1936).

and

$$Y' = \frac{Y}{N}, \qquad Y = 0, \pm 1, \pm 2, \cdots, \pm N,$$

with

$$A(\bar{h}\bar{k}) = A(hk) \qquad B(hk) = -B(\bar{h}\bar{k}).$$

If we write

$$A(X'Y') = \sum_{h=-\infty}^{\infty} \sum_{k=-\infty}^{\infty} A(hk) \cos 2\pi(hX' + kY') \tag{13}$$

and

$$B(X'Y') = \sum_{h=-\infty}^{\infty} \sum_{k=-\infty}^{\infty} B(hk) \sin 2\pi(hX' + kY') \tag{14}$$

then we may write (12) in the form

$$f(X'Y') = A(X'Y') + B(X'Y'). \tag{15}$$

We note that the function $A(X'Y')$ possesses a center of symmetry at the origin, and that the operation of a center at the origin reproduces $B(X'Y')$ with a reversal of sign. We need only compute these two functions for points covering one half of the unit cell. If the function $f(X'Y')$ has a center of symmetry at the origin, we must have $f(X'Y') = f(\bar{X}'\bar{Y}')$ and consequently $B(X'Y') = 0$ everywhere and $B(hk) = 0$ for all values of h and k.

The summations (13) and (14) are now split up into one-dimensional summations following the method suggested by Beevers and Lipson.[2] We shall discuss the expression (13) first. It may be written

$$\begin{aligned} A(X'Y') &= \sum_{h=-\infty}^{\infty} \sum_{k=-\infty}^{\infty} A(hk)\{\cos 2\pi hX' \cos 2\pi kY' - \sin 2\pi hX' \sin 2\pi kY'\} \\ &= C(X'Y') - S(X'Y'), \end{aligned} \tag{16}$$

in which

$$C(X'Y') = \sum_{h=0}^{\infty} \sum_{k=0}^{\infty} C(hk) \cos 2\pi hX' \cos 2\pi kY' \tag{17}$$

with

$$\begin{aligned} &C(00) = A(00), \qquad C(h0) = 2A(h0), \qquad C(0k) = 2A(0k), \\ &C(hk) = 2A(hk) + 2A(\bar{h}k), \end{aligned} \tag{17'}$$

and

$$S(X'Y') = \sum_{h=1}^{\infty} \sum_{k=1}^{\infty} S(hk) \sin 2\pi hX' \sin 2\pi kY' \tag{18}$$

with

$$S(hk) = 2A(hk) - 2A(\bar{h}k). \tag{18'}$$

The expression (17) may now be summed completely. We may sum first with respect to h, or with respect to k as we wish.[11] Suppose we sum with respect to k first. Thus (17) may be written

---

[11] It is usual to sum first over the index that has the highest value represented among the values $C(hk)$; in this way, the number of initial summations to be performed is made as small as possible.

$$C(X'Y') = \sum_{h=0}^{\infty} \mathrm{c}(hY') \cos 2\pi hX' \tag{19}$$

in which

$$\mathrm{c}(hY') = \sum_{k=0}^{\infty} C(hk) \cos 2\pi kY'. \tag{20}$$

We can compute this latter series by the methods described earlier, and use the results of this computation as coefficients in performing the computation (19) by the same methods. This process will be described in detail below.

The summation $S(X'Y')$ may be split up in exactly the same way, i.e.,

$$S(X'Y') = \sum_{h=1}^{\infty} \mathrm{s}(hY') \sin 2\pi hX' \tag{21}$$

in which

$$\mathrm{s}(hY') = \sum_{k=1}^{\infty} S(hk) \sin 2\pi kY'. \tag{22}$$

The series for $B(X'Y')$ may be written

$$\begin{aligned} B(X'Y') &= \sum_{h=-\infty}^{\infty} \sum_{k=-\infty}^{\infty} B(hk)\{\sin 2\pi hX' \cos 2\pi kY' + \cos 2\pi hX' \sin 2\pi kY'\} \\ &= SC(X'Y') + CS(X'Y') \end{aligned} \tag{23}$$

in which

$$SC(X'Y') = \sum_{h=0}^{\infty} \sum_{k=0}^{\infty} SC(hk) \sin 2\pi hX' \cos 2\pi kY' \tag{24}$$

$$CS(X'Y') = \sum_{h=0}^{\infty} \sum_{k=0}^{\infty} CS(hk) \cos 2\pi hX' \sin 2\pi kY'. \tag{25}$$

In these expressions the coefficients are related to the $B(hk)$ by the relations

$$\begin{aligned} &SC(0k) = SC(00) = CS(h0) = CS(00) = 0, \\ &SC(h0) = 2B(h0), \qquad SC(hk) = 2B(hk) + 2B(h\bar{k}) \\ &CS(0k) = 2B(0k), \qquad CS(hk) = 2B(hk) - 2B(h\bar{k}). \end{aligned} \tag{26}$$

The two sums (24) and (25) can now be split up into one-dimensional series in strict analogy with the process described for the series (17) and (18). We shall give no further discussion of the series $B(X'Y')$ in this paper since most two-dimensional series met with in crystal analysis have a center of symmetry, in which case $B(X'Y')=0$. If the need for it arise, the reader, who has made himself familiar with the summation of series of the type $A(X'Y')$, will have no difficulty in setting up a scheme for $B(X'Y')$.

6. *Arrangement of numerical work*

A scheme for the computation of a series of the type $A(X'Y')$ is shown in Fig. 6. The quantities $A(hk)$ are assumed to be known either from ex-

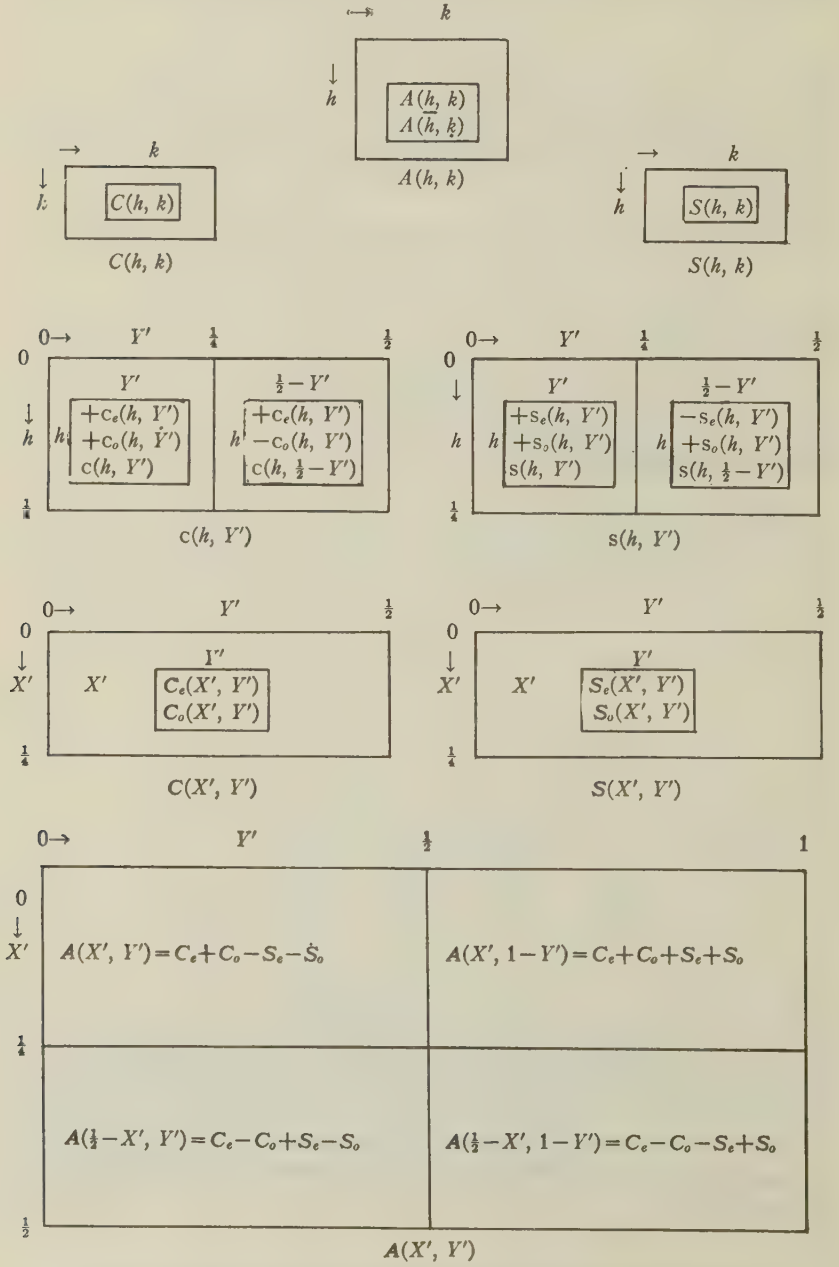

FIG. 6. Arrangement of numerical work for two dimensional cosine series.

periment or as a result of a previous calculation.[12] In general $A(\bar{h}k)$ will be different from $A(hk)$, but $A(\bar{h}\bar{k})$ will be equal to $A(hk)$. The value of $A(hk)$ can thus be entered in a table in which the indices h and k run from 0 to the largest value of h or k for which $A(hk)$ has significance, provided $A(hk)$ and $A(\bar{h}k)$ are written in the same box one above the other. The two tables $C(hk)$ and $S(hk)$ are then constructed from the $A(hk)$ values according to the rules of equations (17′) and (18′) which define these quantities. The table $C(hk)$ provides the material for the summation which leads to $\mathbf{C}(X'Y')$. The first step is a summation over k given by equation. (20). There will be as many such series to sum as there are values of h, and each series will be summed for the points 0 to $N/4$. The results of this summation are entered in the $\mathrm{c}(hY')$ table. The summations for the even k values lead to the quantities $\mathrm{c}_e(hY')$ and those for odd k lead to $\mathrm{c}_o(hY')$. Both these sets of quantities are entered in the same box in the table, and their sum gives the values of $\mathrm{c}(hY')$ for Y' values from 0 to $N/4$. This table is now extended to $N/2$ by writing $\mathrm{c}_e(hY')$ and $-\mathrm{c}_o(hY')$ in the $N/2-Y'$ box, the sum of these two quantities being the value of $\mathrm{c}(h, \overline{N/2-Y'})$.

We must now sum $(N/2+1)$ series of the type (19) for the points 0 to $N/4$. The results of these summations, i.e. $\mathbf{C}_e(X'Y')$ and $\mathbf{C}_o(X'Y')$ are entered in the same box in the $\mathbf{C}(X'Y')$ tables and their sum in each case then gives the $\mathbf{C}(X'Y')$ values for the points in question.

A similar procedure now leads to a computation of the table $\mathbf{S}(X'Y')$ from the table $S(hk)$, the only difference being in the use of sine stencils instead of cosine stencils and in the rules for combination of the even and odd parts of the various sums. In the final table, according to equation (16) the function $\mathbf{A}(X'Y')$ is formed by subtracting $\mathbf{S}(X'Y')$ from $\mathbf{C}(X'Y')$ while the values at the points $(X', N-Y')$ are obtained by adding these two quantities.[13]

The reader who finds it necessary to sum a series that does not possess a center of symmetry, and must therefore sum the series $\mathbf{B}(X'Y')$ given by equation (14), will find no difficulty in setting up a scheme entirely

[12] $A(hk)$ may be either the structure factor F or the square of the absolute value of the structure factor. The magnitudes of the structure factors can be determined from measurements of the intensities of the diffracted x-ray beams from the crystal planes. The signs of the absolute values of the structure factors are not determinable by measurement, however, and must be obtained from a previous solution, either by trial and error, or by the use of an $|F|^2$ series, or, in some cases, by comparison with those of another member of the same isomorphous series of crystals.

[13] Since the tables of $\mathbf{C}_e(X'Y')$, $\mathbf{C}_o(X'Y')$ and $\mathbf{S}_e(X'Y')$, $\mathbf{S}_o(X'Y')$ are always the same size (for a given number of divisions in the unit cell e.g. 48 or 60) a strip of cardboard with 2 suitable notches can be used to select quickly the four values needed for combination into the final value of $\mathbf{A}(X'Y')$. This device was first used in these summations by Mrs. Selma Blazer Brody and we are indebted to her for the suggestion.

analogous to that of Fig. 6. The difference will lie in a different use of stencils and a different combination procedure. Equations (23) to (26) and the results of equations (5) and (9) provide all the information necessary for the purpose.

The computation outlined in Fig. 6 can conveniently be carried out on squared paper of dimensions 50 cm. × 75 cm. ruled in 1 cm. squares. Since the three numbers required in one entry in the tables $\mathrm{c}(hY')$, $\mathrm{s}(hY')$, etc. can readily be entered in a 1 cm. square, the whole computation with the exception of the final $\boldsymbol{A}(X'Y')$ table can be entered on one sheet. The $\boldsymbol{A}(X'Y')$ table then occupies a separate sheet.

7. *Conclusion*

In this paper, we have described in detail a method for the summation of one dimensional Fourier series[14] and a procedure that enables this method to be applied to the summation of two-dimensional series. In conclusion it is perhaps desirable to make a brief comparison between this method and the two others which have been described previously. The method of Robertson[3] and the present method are the same in principle, but in practice they differ in one important point. In Robertson's method the strips are mounted in slides. Each slide is set for a given X' value by means of an indicator. The advantage of his method is that the numbers to be added appear in a vertical column, and can be added with maximum ease. In the method we have described the selection of numbers is by means of stencils, and the addition is along a slanting or zigzag sequence of holes. Owing to the relatively small number of holes in any one stencil, this adds little or no difficulty to the process of addition. In going from one point to the next, in Robertson's method all the strips must be individually reset, whereas in the method here described it is only necessary to replace one stencil by another.

The method of Lipson and Beevers[4] differs quite radically from the other two[3,5] in that their strips carry the values

$$D \cos 2\pi hX/N \quad \text{and} \quad D \sin 2\pi hX/N$$

for fixed values of h and for varying values of X. Strips for sine or cosine are then selected for a given D and its appropriate h. After the strips have been selected, they are arranged one above the other and the figures in vertical columns are simply added. If positive and negative values are both present they must be added separately and the results combined.

---

[14] Those familiar with the processes of Fourier analysis will have no difficulty in recognizing that the method is equally applicable to Fourier analysis by the method of equidistant ordinates. Cf. Whittaker and Robinson: The Calculus of Observations, Blackie, London (**1924**), and Eagle, A.: Fourier's Theorem, Longmans, Green, London (**1925**).

The Lipson and Beevers method thus requires very many more strips than are required by the present method. This disadvantage is, however, somewhat reduced by the fact that strips for the numbers 1 to 100 have been printed and are available. In the method of Lipson and Beevers, the Miller index, the *D*-value with its sign, and the nature of the function (sine or cosine) all must be watched in the selection of the strip; whereas in the method described here, only the *D*-value with its positive or negative sign determines the selection. A comparison of the experience of workers using the Lipson-Beevers method and of those using the one under discussion here, seems to indicate that the time taken for a summation is not greatly different for *D*-values ranging from 0 to 100. For *D*-values ranging from 0 to 1000, or more, the method of Lipson and Beevers would require such an enormous number of strips that it would not be so convenient as the stencil method, which experience has shown to be well adapted to this range.[15]

ACKNOWLEDGMENT

The authors desire to thank Professor J. D. H. Donnay of Université Laval for reading the manuscript of this paper and to express their appreciation to Mr. J. H. Snapp of the Geophysical Laboratory for making the photographs.

---

[15] Sets of 1800 strips (*F*-values 0 to 300, negative and positive, three strips of each kind) for use with the method described in this paper may be obtained from Prof. J. D. H. Donnay, Institut de Géologie et de Minéralogie, Boulevard de l'Entente, Québec, P. Q., Canada. (Price $9.00 per set.)

THE SYSTEM CaO-SiO_2-P_2O_5

Richard L. Barrett,
Case School of Applied Science, Cleveland, Ohio
and
William J. McCaughey,
Ohio State University, Columbus, Ohio.

Abstract

The system contains, in addition to the binary phases previously described in the literature, two ternary phases, nagelschmidtite and silicocarnotite, which have been known as constituents of certain slags. The equilibrium diagram presents some features of special interest. The field of cristobalite is very large. There is an extensive region of liquid immiscibility in which two liquids in equilibrium with cristobalite are formed. Very extensive solid solution prevails in the four phases, calcium orthosilicate, nagelschmidtite, silicocarnotite, and tricalcium phosphate, which form a binary system with the first and last named as end members. Calcium orthosilicate may contain up to 10% P_2O_5 in solid solution, and nagelschmidtite, the formula for which may be expressed as $Ca_7Si_2P_2O_{16}$, can have a P_2O_5 content varying between 12% and 24%. The solid solution seems to be of the substitution sort with PO_4 replacing SiO_4 groups. In both phases refractive indices decrease as P_2O_5 content increases.

Introduction

The system CaO-SiO_2-P_2O_5 is of greater interest to the mineral technologist than to the student of igneous rocks for reasons which will be considered later in this paper. The system has been the subject of study by chemists and metallurgists for more than fifty years, at first in connection with the "Thomas" or basic Bessemer process of steel making and, more recently, through attempts to develop new methods for producing high grade phosphatic fertilizers. Although many investigators have worked in this field, the fundamental equilibrium relationships have never been worked out, and not even a tentative equilibrium diagram has ever been presented. It is the purpose of this paper to supply this omission in some degree, with the hope that a better understanding of this system may further our knowledge of basic steel making reactions and perhaps contribute something of value to ceramics, glassmaking, or other related industries.

Historical

The pioneer work in the study of this system was done in the 1880's by Hilgenstock (13) (14), Carnot and Richards (6), and Stead and Risdale (31). These investigators, working independently, studied carefully selected crystals from slowly cooled "Thomas" slags and published chemical analyses and crystallographic data. In addition to some iron-bearing phases, they established the presence of tetracalcium phosphate, an apatite-like phase, and a calcium silico-phosphate, the generally accepted formula for which is $5\ CaO \cdot SiO_2 \cdot P_2O_5$. Kroll in 1911 (18) summarized the work of the aforementioned investigators and named the three phases after their discoverers, respectively, hilgenstockite, steadite, and silicocarnotite. The latter name seems highly unfortunate in view of the fact that the name carnotite has been given to an entirely different mineral. However, the word silicocarnotite has now been used by so many different writers, that it seems firmly entrenched in the literature and must perforce be accepted.

H. Blome (3) and O. Nielson (24) in 1910 and 1913 investigated synthetic preparations in this system by chemical means. Their data are of some interest, but they lacked a suitable means of phase identification and consequently came to conclusions not in accord with more recent investigations.

In more recent times a number of workers have studied "Thomas" and open hearth slags by means of the petrographic microscope. Scott and McArthur (30) published the results of their investigation in 1922. In addition to an oxide phase which does not concern us here, they found three silico-phosphate phases. Their descriptions do not include complete optical data and they attempted to arrive at the composition of the phases by inference from the analyses of the slags themselves. The compositions they give do not correspond exactly to those recognized in this paper, but the phases described appear to be silicocarnotite, an apatite, and the phase later described by Nagelschmidt (23) from an English slag.

Schneiderhöhn (28) (29) has in recent years made an extensive petrographic study of various basic slags, mainly by the examination of polished sections, but also in part by the use of thin sections and fine powders. In normal "Thomas" slags he found three phases which he identified as tetracalcium phosphate, silicocarnotite, and a dark phase consisting of mixed oxides. In a slag to which sand had been added, only the last two phases were found. Reheating and slow cooling produced no change in constitution, indicating that equilibrium conditions prevailed in the slags studied. The citrate solubility content varied with the amount of silicocarnotite. Schneiderhöhn examined various other ,'Thomas" slags of varying composition with results similar to those indicated acove. He found, however, that slags to which $1\frac{1}{2}$ per cent CaF_2 had been added in the converter, contained no silicocarnotite, having in its place apatite and beta dicalcium silicate. Open hearth slags of various compositions ranging from 8 per cent to 26 per cent P_2O_5 were also examined. Schneiderhöhn found silicocarnotite in most of these slags and in addition three phases whose compositions were unknown.

He states that two of these phases contain phosphorus and the third he believes to be a silicate. Open hearth slags to which fluorspar had been added contained apatite but dicalcium silicate was not observed. Plates showing polished sections of various slags were included in this paper.

Nagelschmidt (23) in 1937 reported a phase having the composition $7CaO \cdot 2SiO_2 \cdot P_2O_5$ which he recovered by specific gravity separation from an English basic open hearth slag. He gives the optical properties of this phase and shows that it is distinct from silicocarnotite by a comparison of *x*-ray diffraction patterns. Apparently it did not occur to him to distinguish this phase from dicalcium silicate, or a solid solution of it, but a comparison of diffraction patterns shows distinct differences.

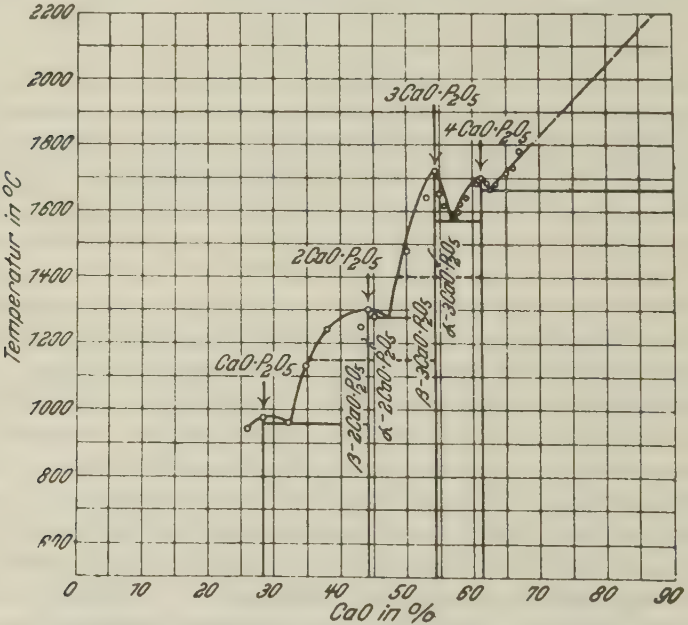

FIG. 1. System CaO-P_2O_5 from Körber and Trömel, *Arch. Eisenhüttenwesen* **1**, 7 (1933).

The equilibrium diagram for the two-component system CaO-SiO_2 was published by Rankin and Wright (25) in 1915 and revised by Ferguson and Merwin (8) (9) in 1919. This work is well known in American literature and need not be summarized here.

Bredig, Franck, and Füldner (4) (5) and Körber and Trömel (16) (17) (32) in 1932 and 1933 published phase diagrams for part of the two-component system CaO-P_2O_5. These writers find the following phases: $4CaO \cdot P_2O_5$, two crystal modifications of $3CaO \cdot P_2O_5$, and two crystal modifications of $2CaO \cdot P_2O_5$, and $CaO \cdot P_2O_5$. The final papers of the two groups of writers are in essential agreement and Fig. 1, taken from Körber and Trömel's paper, shows the equilibrium relationships found. They also give *x*-ray diffraction patterns for the phases and in a paper by Trömel (32) there is a description of the optical properties as determined by Hans Schneiderhöhn.

In their first efforts, Bredig, Franck, and Füldner failed to exclude water vapor and they were obliged to retract and revise the first equilibrium diagram they published. It was found that an apatite phase was formed at temperatures as high as 900° C. in even slightly moist air, but if water vapor was rigidly excluded no apatite phase occurred. In this connection it is worth noting that the apatite structure readily permits the substitution of various ions, and apatites occur with a wide range of compositions, as has been shown by Gruner and McConnell (11), McConnell (19) (20) (21), Hendricks, Jefferson, and Mosley (12), and others. There is every indication that the apatite configuration is a very stable one and that other phosphates of not too different compositions are readily converted into apatites where conditions permit. This "reversion" to the apatite structure has been a difficult problem in the production of high grade phosphatic fertilizers. It is particularly noteworthy that Gruner and McConnell found that the SiO_4 group could substitute for the PO_4 group in the apatite structure as it will be shown in this paper that extensive solid solutions involving this type of substitution prevails in the CaO-SiO_2-P_2O_5 system. Trömel (33) has given cogent reasons for the nonexistence of a pure "oxyapatite" and no such phase is found in either the two-component system, CaO-P_2O_5 or the three-component system, CaO-SiO_2-P_2O_5, when water is carefully excluded. Hydroxyl apatite, however, is readily formed and apparently may exist with less than the theoretical amount of water.

Behrendt and Wentrup (2) studied a portion of the three-component system between the CaO-P_2O_5 join and silicocarnotite by means of cooling curves. Their determinations of transition temperatures are of interest but were not supplemented by any identification of phases.

Hill, Hendricks, Jefferson and Reynolds (15) have studied a small part of the three-component system in connection with the defluorination of rock phosphates in fertilizer manufacture. This subject has been much investigated by these writers and others of the Bureau of Soils of the U. S. Department of Agriculture. Their preparations were held at 1400° C. (below the liquidus). The phases they found were tricalcium phosphate, an apatite phase, and an unidentified phase having a composition probably intermediate between silicocarnotite and tricalcium phosphate. The unidentified phase which these writers call phase "B" they believe to be identical with the phase described by Bredig, Franck, and Füldner as being formed in place of silicocarnotite where the time of heating was too short or the temperature was below 1400° C., and designated by them as phase "X." The writers have not encountered this phase in their own work which was mainly carried to the temperature of the liquidus.

Körber and Trömel (17) state that in 1930 the Kaiser-Wilhelm-Institut für Eisenforschung began a "planmässige" thermal and microscopic study of the system CaO-P_2O_5-SiO_2. By 1933 they had published the diagram for the CaO-P_2O_5 system already mentioned as Fig. 1 and in one paper (17) they gave the preliminary sketch of the three-component system reproduced here as Fig. 2. Since 1933 they have published nothing further in this field.

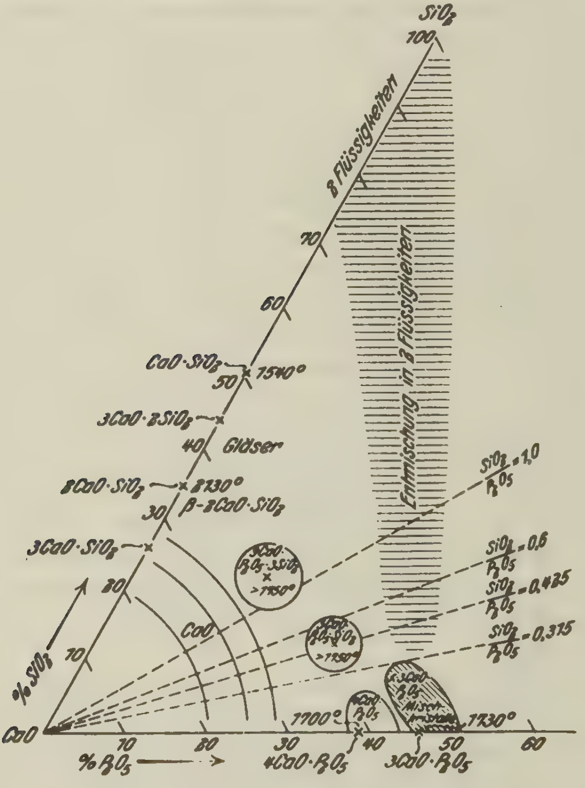

FIG. 2. Sketch for system CaO-P_2O_5-SiO_2 from Körber and Trömel, *Arch. Eisenhüttenwesen*, **1**, 7 (1933).

Many other papers dealing with phosphates of lime, structure of teeth and bones, phosphatic fertilizers, etc., have been published. These are well summarized by Eisenberger, Lehrman and Turner (7) and are not mentioned here because, for the most part, they are only of indirect interest in connection with the purposes of our investigation.

EXPERIMENTAL PROCEDURE

The investigations were begun with a general survey of the system to determine what phases are present, and to define the approximate field boundaries of the various phases.

Compositions varying, for the most part, at 5 per cent intervals for each of the three components were prepared, although in a number of cases intermediate compositions were also studied. Raw materials were thoroughly calcined, silicic acid for the SiO_2, calcined $CaHPO_4$ for $Ca_2P_2O_7$, and precipitated $CaCO_3$ for CaO, all reagents being "Bakers Analyzed."*

After weighing, the batches were given a preliminary mixing by shaking in a glass jar and then were ground in a porcelain mortar for about half an hour. They were then molded with water into cylinders about $\frac{1}{2} \times 1$ inch. At first a little dextrine was used to bind the ingredients, but this proved to be unnecessary and was eliminated.

The cylinders were then calcined, reground and remolded wet to further promote intimate contact of the ingredients. Best results were obtained when this preliminary calcining was carried on at about 1000° C., rather than at higher temperatures. This procedure evidently drives off the CO_2 from the $CaCO_3$ without inducing much combination between the lime and silica. The calcined material evolves considerable heat as it hydrates, and the hydrated lime thus produced seems to come into intimate contact with the grains of the other materials and thus promotes more complete combination during the subsequent procedures.

As is well known, calcium phosphates are readily reduced at high temperatures in the presence of carbon. Nielson (24) found that CO did not reduce phosphates at the temperatures he studied. However, we experimented with an Ajax-Northrup induction furnace using a graphite crucible, and also tried a "Norbide" crucible in an effort to obtain controlled high temperatures. Although the samples were not permitted to touch the crucibles, and the crucibles were left partly uncovered to permit ready access of air, the evolution of a dense white smoke indicated reduction of the phosphates. Accordingly, we have been particular to maintain oxidizing conditions in all heating operations.

---

* In some of our earlier experiments $Ca_3(PO_4)_2$ purchased from chemical supply houses was used. This material proved to contain more lime than the formula composition, and when fused yielded an apatite. It appears to be a finely divided form of hydroxyl-apatite. The calcined $CaHPO_4$, on the other hand, proved to be a reliable source of P_2O_5.

The furnace used for most of our work was a "Globar" resistance furnace which was capable of a temperature of 1550° C. and controlled by a "Micromax" controller. The samples, in the form of small cylinders, rested on a magnesite slab and, after heating, the portion which had been in contact with the slab was discarded. Where any apparent tendency to react with the magnesite was found, the sample was placed on a piece of platinum foil.

In the part of the system which was of most interest to us, liquidus temperatures were too high to be attained in this furnace. Accordingly, other samples were fused in an oxy-acetylene flame. One of the small cylinders was placed on a magnesite slab and the flame from an oxy-acetylene torch was played on its top. Care was taken to avoid contact with the reducing portion of the flame and only the top of the cylinder was fused, making a small pool of melt resting on the unfused portion of the cylinder. As soon as the flame was removed, the samples cooled very rapidly and on microscopic examination the melted portion usually proved to consist of one phase, or of one phase plus a glass.

All of the samples were examined under the petrographic microscope by the immersion method and the refractive indices and other optical properties of all phases observed were determined. Although some of the phases are rather similar in their optical properties and some show considerable variation due to solid solution, phase identification could be made with considerable assurance, once the range of variation had been determined.

X-ray diffraction patterns were made for each phase and, wherever it seemed desirable, phase identification was checked by a comparison of diffraction patterns. The *x*-ray studies were made by the powder method on a General Electric apparatus employing molybdenum radiation and a camera radius of 20 cm. The films were measured and interplanar spacings for each of the lines were calculated.

Through the kindness of Prof. A. S. Coffinberry of the Department of Metallurgy of Notre Dame University, *x*-ray films for calcium orthosilicate, nagelschmidtite, silicocarnotite, tricalcium phosphate, and tetracalcium phosphate were made using copper radiation and a camera radius of 57.2 mm. For purposes of visual comparison these films are reproduced in Fig. 6.

Equilibrium Diagrams

The high melting temperatures prevailing in that portion of the system of most interest to us precluded the use of the platinum quenching furnace commonly employed in work of this sort. The somewhat crude expedient of melting in the oxy-acetylene flame permits the approximate mapping of field boundaries, although temperature measurements with the optical pyrometer under these conditions are only rough approximations. The accompanying diagram, Fig. 3, shows the field boundaries of the various phases as mapped by this means.

Because the high liquidus temperatures precluded accurate measurement by the usual means, this diagram is presented without isotherms. However, we believe it represents the essential equilibrium relationships between the various phases and it embodies the principal contribution of the present paper. The directions of falling temperature and the character of crystallization can always be inferred from such an equilibrium diagram without the aid of isothermal lines, or any table of temperatures. However, for the convenience of the reader in visualizing the form of the liquidus surfaces, a table is appended to the diagram giving the approximate temperatures for the various points. The presence of additional components may be expected to affect the equilibrium relationships. However, examination of a number of steel-making slags indicates that the essential relationships are not altered by the presence of iron and manganese oxides as long as CaF_2 is not present. Consequently, it may

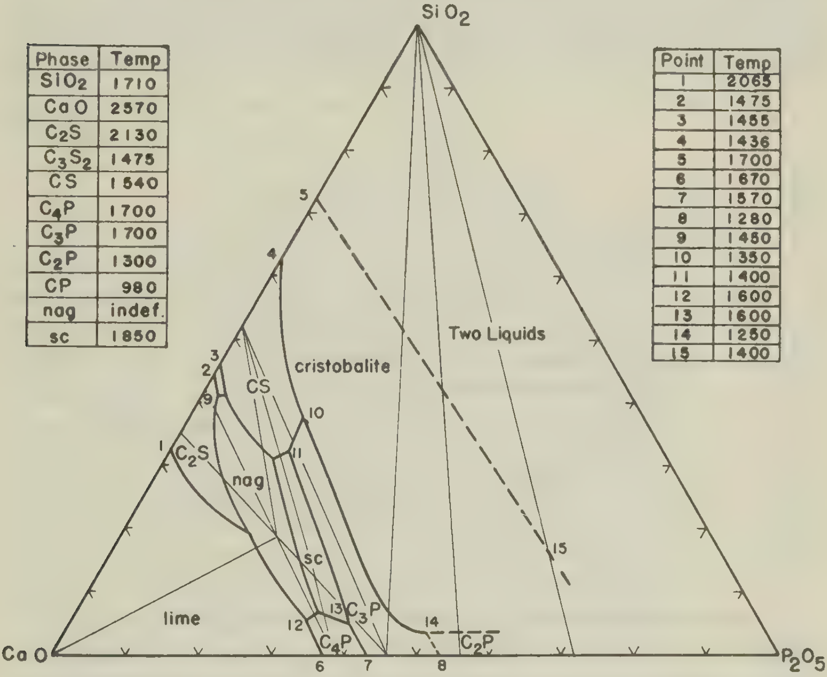

Phase	Temp
SiO_2	1710
CaO	2570
C_2S	2130
C_3S_2	1475
CS	1540
C_4P	1700
C_3P	1700
C_2P	1300
CP	980
nag	indef.
sc	1850

Point	Temp
1	2065
2	1475
3	1455
4	1436
5	1700
6	1670
7	1570
8	1280
9	1450
10	1350
11	1400
12	1600
13	1600
14	1250
15	1400

FIG. 3. Equilibrium diagram for the system CaO-SiO_2-P_2O_5. Temperatures are approximate.

be anticipated that this equilibrium diagram will be useful in furthering our understanding of the steel-making process.

Several years ago, in the course of some microscopic examinations of open hearth steel slags, the writers noticed that the dicalcium silicate phase in the slag had lower refractive indices and lower birefringence than the pure compound. Further investigation suggested that the change in indices was due to the presence of P_2O_5 in solid solution. This probability was confirmed by the fact that in the course of the present investigation it was found that dicalcium silicate occurring in preparations containing P_2O_5 always has lowered indices and birefringence. Since a similar but even greater variation in optical properties was found in the ternary compound we have called nagelschmidtite, a series of compositions intermediate between dicalcium silicate and tricalcium phosphate was prepared and brought as nearly as possible to equilibrium at 1550° C. Microscopic examination of these preparations showed that over a considerable range of compositions only one phase is present and that there is a considerable variation in properties of this phase. The results of this investigation are shown in Fig. 4 in the form of a tentative equilibrium diagram for the binary system dicalcium silicate-tricalcium phosphate. Because of the very high temperatures involved

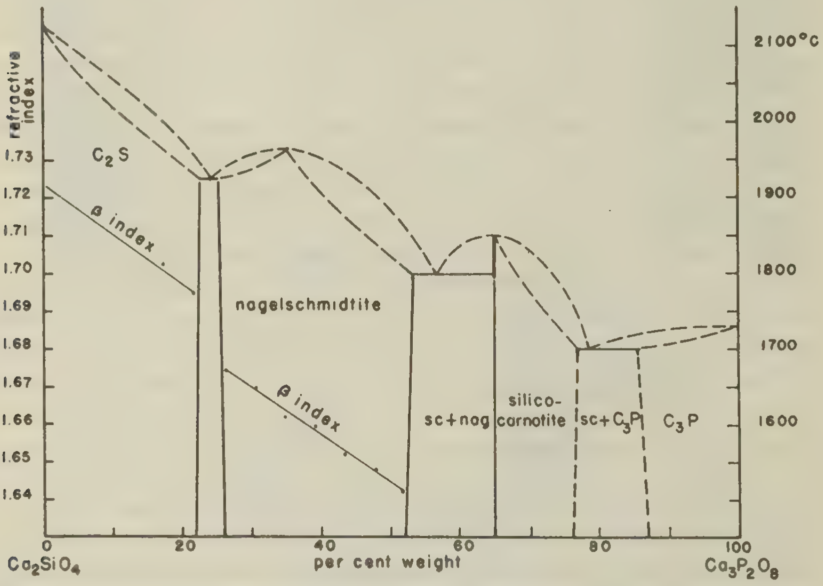

FIG. 4. Diagram showing probable equilibrium relationships in the system Ca_2SiO_4-$Ca_3P_2O_8$. Liquidus temperatures not definitely known. Extent of solid solution and variation in refractive index shown for calcium orthosilicate and nagelschmidtite.

and the consequent difficulty of making accurate temperature measurements the liquidus lines are diagrammatic. However, the diagram probably shows the essential equilibrium relationships. The limits of solid solution for dicalcium silicate and nagelschmidtite are shown and the relationship between refractive index and composition for the β ray for those two phases is plotted. It will be noted that the homogeneity ranges for these two phases very nearly meet, and that the refractive index curves for the two phases are practically parallel straight lines. These facts are suggestive of the probable structural relationship between these two phases which is discussed later. The phenomenon of solid solution in silicocarnotite and tricalcium phosphate was not studied in detail and the homogeneity ranges shown for these phases are taken from the work of Hill, Hendricks, Jefferson and Reynolds (15).

Discussion of the Phases

Blome (3), Scott and McArthur (30), Schneiderhöhn (28) (29), and Körber and Trömel (17), have all suggested the existence of a silicophosphate having a higher SiO_2/P_2O_5 ratio than silicocarnotite. However, the first investigator to isolate such a phase and describe its physical properties was Nagelschmidt, in 1937 (23). He reported separating this phase from an English basic open hearth slag by using specific gravity methods. Accordingly, we have given this phase the name nagelschmidtite, since this name, cumbersome as it is, is easier to handle than the chemical formula. This phase is described by Nagelschmidt as being biaxial (+), $\alpha = 1.652$, $\gamma = 1.661$, parallel extinction, $G. = 3.035$. The chemical analysis corresponds closely to the formula $7CaO \cdot 2SiO_2 \cdot P_2O_5$. The phase as prepared by us has an optic angle of about 20° and a birefringence of about 0.004. The higher birefringence reported by Nagelschmidt may perhaps be due to solid solution. The present investigation shows that in the three-component system this phase has a rather large field and a considerable homogeneity range, refractive indices varying between a maximum of 1.675 and a minimum of 1.642 for the β ray, the optic angle varying between 20° and practically zero.

Because of its lowered indices and birefringence dicalcium silicate containing P_2O_5 is rather difficult to distinguish from nagelschmidtite by microscopic means alone. However, with the aid of the x-ray diffraction pattern the distinction can be made with certainty.

Silicocarnotite, $5CaO \cdot SiO_2 \cdot P_2O_5$, is given by numerous investigators as the principal constituent of "Thomas" slags and as the cause of its solubility in citric acid, which is used as a test of the availability of the phosphorus for a fertilizer. It is the blue pleochroic phase described by Stead and Risdale (31). The process for the defluorination of phosphate rock by heating in the presence of silica, aims at its conversion as completely as possible to silicocarnotite. Since upon slow cooling, in a moist atmosphere, there is a tendency to "revert" to the apatite structure, the range of compositions between silicocarnotite and tricalcium phosphate has been the subject of considerable study by the U. S. Bureau of Soils. Hill, Hendricks, Jefferson, and Reynolds (15) state their findings resulting from these studies, and they and others at the Bureau of Soils have published a number of papers on various phases of the fertilizer problem. The portion of Fig. 4 showing the homogeneity ranges of silicocarnotite and tricalcium phosphate is adapted from their paper.

It is difficult to prepare well crystallized silicocarnotite from the pure constituents, but the growth of crystals is facilitated in a slag. We held a sample of the high phosphorus open hearth slag from Ensley, Alabama, at 1525° C. for 40 minutes and then slowly cooled it to 1400° C. Upon examination it proved to consist mainly of well crystallized silicocarnotite. Another sample of slag from the same mills and given the same treatment contained both silicocarnotite and nagelschmidtite. Figure 5 is a photomicrograph of a thin section of this slag. The two phases may be readily distinguished between crossed nicols by the pronounced difference in birefringence.

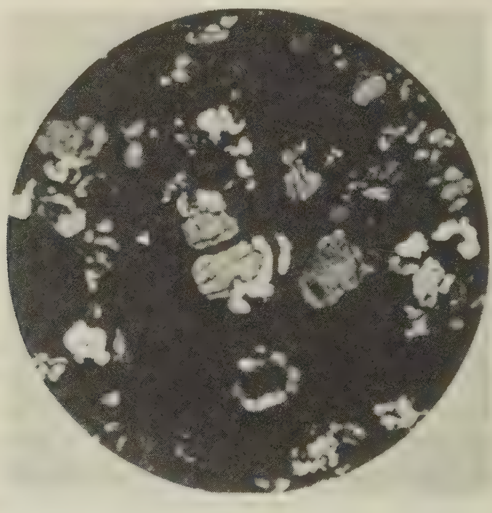

FIG. 5. Photomicrograph of thin section of remelted open hearth slag from Ensley Alabama. Magnification about 75 times. Crossed nicols. Gray grains are nagelschmidtite white grains are silicocarnotite. Background is dark colored interstitial phase.

Silicocarnotite is readily recognized by its optical properties and diffraction pattern. It is biaxial with $2V$ nearly 90°. Because of the large optic angle the sign is often indeterminate, but in most samples appears to be (+). The refractive indices are: $\alpha=1.632$, $\beta=1.636$, $\gamma=1.640$. Hill and his co-workers (15) found it to have a homogeneity range in the direction of tricalcium phosphate as shown in Fig. 4.

Tricalcium phosphate (hereafter abbreviated C_3P) has a rather surprisingly large field in the three component system. The α form is biaxial (+), $2V$ about 70°, $\alpha=1.588$, $\gamma=1.591$. It inverts to the β form at about 1400° C., according to Körber and Trömel (15). Hill and his co-workers found that the inversion became very slow when silica was present in the lattice, the homogeneity range being as shown in Fig. 4. The presence of silica in solid solution can increase the refractive index to a maximum of about 1.615. The β form of tricalcium phosphate seems to be identical with the mineral whitlockite, described recently by Frondel (10).

Tetracalcium phosphate (hereafter abbreviated C_4P) was found by Hilgenstock (13) (14), Stead and Risdale (31), and others in "Thomas" slags nearly 60 years ago. It is readily synthesized by fusing the appropriate composition. It is biaxial (+), $2V$ about 30°, and is characterized by polysynthetic twinning, similar in appearance to that of the plagioclase feldspars. The refractive indices are: $\alpha=1.650$, $\beta=1.651$, $\gamma=1.656$. The field of the phase is small. Solid solution, if it exists, is of very limited extent.

Calcium pyrophosphate (hereafter abbreviated C_2P) is readily prepared by calcining dicalcium hydrogen phopshate. Like C_3P it has an α and β modification with an inversion temperature of about 1150° C., as determined by Körber and Trömel in their study of the $CaO-P_2O_5$ system. The α form is biaxial (−) with small to moderate optic angle, $\alpha=1.585$, $\gamma=1.605$.

Pseudowollastonite (hereafter abbreviated CS) has an extensive field in the system. It is easily distinguished from neighboring phases by its higher birefringence. It apparently does not take P_2O_5 into solid solution at all, since no apparent variation in its optical properties occurs in the system.

CaP_2O_6 can be readily prepared by heating $CaH_4(PO_4)_2 \cdot H_2O$. It is biaxial (−) with $2V$ about 60°. The refractive indices are: $\alpha=1.578$, $\beta=1.588$, $\gamma=1.593$. Except for somewhat larger optic angle and lower indices it appears under the microscope quite similar to C_2P.

LIQUID IMMISCIBILITY

The most striking fact about Fig. 3 is the very large size of the field of cristobalite. A melt of composition CaO 50 per cent, P_2O_5 45 per cent, SiO_2 5 per cent crystallized to α-C_3P but contained many small radiating inclusions of cristobalite which were clearly the first crystals to form. These inclusions are usually spherulitic in character and being nearly isotropic they suggest the globular, glassy inclusions formed by the freezing of immiscible liquids. As a matter of fact, Körber and Trömel in their diagram, which we are reproducing as Fig. 2, indicate that the region of liquid immiscibility extends down into this area. However, in the case of immiscible liquids both liquids must be in equilibrium with the same crystal phase. If those spherulites were formed from the devitrification of globules of highly siliceous liquid, the host liquid would also have to be in equilibrium with silica. When we examine melts somewhat closer to the CaO-SiO_2 join, we frequently find skeleton crystals of cristobalite with an octahedral development imbedded in a glass. These are clearly primary cristobalite.

The actual region of liquid immiscibility is approximately shown by the dashed line on Fig. 3. We have not attempted to map this region accurately or to determine the compositions of the liquids formed. However, the more siliceous glass has a refractive index close to 1.46 in all the melts examined which suggests that its composition is close to pure silica. The temperature at which the two liquids separate is about 1700° C. on the CaO-SiO_2 join according to Grieg, and we found that two liquids formed in a melt of composition CaO 23 per cent, SiO_2 20 per cent, P_2O_5 57 per cent, at about 1400° C. The less siliceous of the two glasses formed in this latter melt has a refractive index of about 1.535.

Because of the volatility of P_2O_5, compositions lying within the composition triangle CaP_2O_6-SiO_2-P_2O_5 require a special technique for study and we have made no attempt to investigate them. However, it is interesting to note that Nielsen (24) reported preparing phases having compositions corresponding to $3SiO_2 \cdot P_2O_5$ and $2SiO_2 \cdot P_2O_5$. He considered these to be definite compounds, but his description of them suggests that they were glasses.

SOLID SOLUTIONS

The most striking result of our investigation is the very extensive solid solution existing in the system calcium orthosilicate-tricalcium phosphate. Not only do the end members have considerable homogeneity ranges, but the two intermediate ternary compounds, nagelschmidtite and silicocarnotite, display the same phenomenon: nagelschmidtite particularly being found with P_2O_5 content varying between 12 per cent and 24 per cent. Unfortunately, the crystal structure of all four of these compounds is unknown and it is not our intent to go into this phase of the problem. However, a few relevant facts may be worth mentioning. As Fig. 6 shows there is a striking general similarity between the diffraction patterns for the four phases which may be indicative of a similarity in crystal structure. The compositions are seen to be analogous if we write them thus:

C_2S	$Ca_{24}Si_{12}O_{48}$
Nagelschmidtite	$Ca_{21}Si_6P_6O_{48}$
Silicocarnotite	$Ca_{20}Si_4P_8O_{48}$
C_3P	$Ca_{18}P_{12}O_{48}$
Type formula	$Ca_{(2\ Si+3/2P)}\ (P,\ Si)_{12}O_{48}$

The PO_4 group is known to be a tetrahedral arrangement with dimensions similar to those of the SiO_4 group, and McConnell (19) has shown that SiO_4 can substitute for PO_4, in apatite, at least to some extent. It seems highly probable then that the solid solution encountered here is of the substitution type with PO_4 substituting for SiO_4 groups. Because of the difference in valence between the two groups, this substitution involves leaving some of the Ca positions in the lattice vacant. One might speculate that if it were not for this fact complete solid solution between the end members would exist, but that the emptying of some of the Ca positions in the lattice brings about structural changes which introduce the two ternary phases into the system.

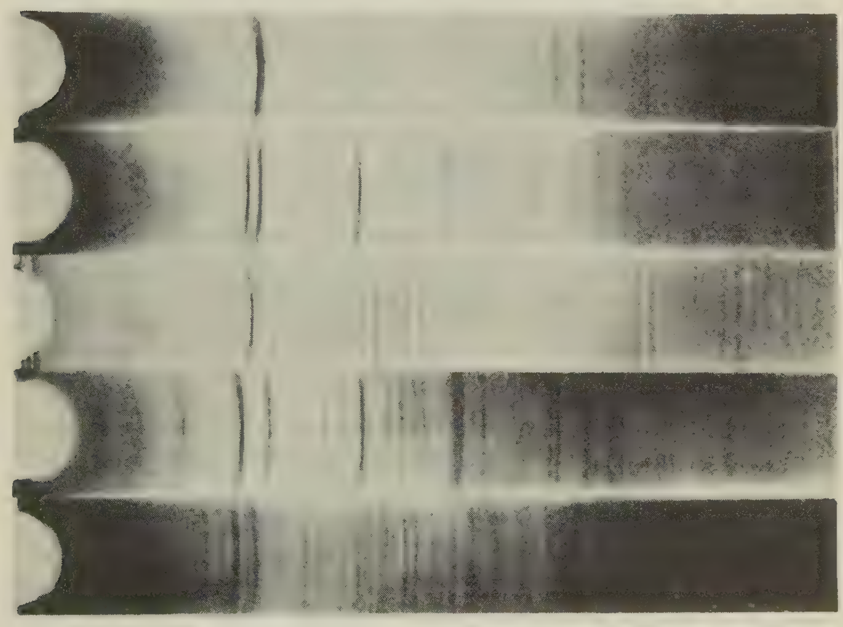

FIG. 6. *X*-ray powder diffraction patterns made with Cu radiation. Reading from top to bottom the phases are: β-calcium orthosilicate, nagelschmidtite, silicocarnotite, α-tricalcium phosphate, and tetracalcium phosphate.

It is notable that neither CS nor C_2P show appreciable homogeneity ranges. It appears that solid solution between the calcium silicates and calcium phosphates is limited to the orthosilicate ratio. According to the well established rules of silicate structure, the orthosilicate should be characterized by independent SiO_4 groups while the metasilicate would probably have a chain or ring structure of linked SiO_4 groups. It would seem then, that in this system PO_4 groups substitute freely for SiO_4 groups when they are independent, but that the substitution does not occur in the more complex silicate groupings. Certainly isomorphism between silicates and phosphates is not a common phenomenon.

The results of this investigation do not have a very direct bearing on the problem of the igneous rocks because magmas always contain fluorine and hydroxyl ions. There is excellent evidence that the presence of either of these profoundly changes the equilibrium relationships in this system. The formation of hydroxyapatite in the presence of moist air has already been mentioned as have been Schneiderhöhn's observations on slags to which fluorspar had been added.

In the field of mineral technology, however, the importance of this system has long been recognized as shown by the large volume of literature centering around the study of slags and phosphate fertilizers. The results of this investigation should contribute to a better understanding of the part played by basic slags in the elimination of phosphorus from steel in the refining process.

Summary

The equilibrium relationships in the system CaO-SiO_2-P_2O_5 were investigated and an equilibrium diagram prepared. The solid phases were identified by their optical properties as determined by the use of the petrographic microscope, and by their x-ray diffraction patterns.

In addition to the binary compounds previously described in the literature, two ternary phases, nagelschmidtite and silicocarnotite which have been previously known as constituents of certain slags, were found to exist in the system.

The equilibrium diagram presents two special features of particular interest. There is an extensive region of liquid immiscibility in which two liquids in equilibrium with cristobalite are formed. Very extensive solid solution prevails in the four phases, calcium orthosilicate, nagelschmidtite, silicocarnotite, and tricalcium phosphate, which form a binary system with the first and last mentioned as end members. A binary diagram portraying the homogeneity ranges and the variation in refractive indices resulting from solid solution is presented.

ACKNOWLEDGMENTS

Thanks are due to W. A. Klamm and W. G. Hotchkiss who rendered valuable assistance in carrying out this investigation.

REFERENCES

1. Bainbridge F., Iron & Steel Inst. (London): *Carnegie Scol. Mem.*, **10,** 1–40 (1920).
2. Behrendt, G., and Wentrup, H., *Arch. Eisenhüttenwesen*, 95–102 (1933).
3. Blome, H., Stahl und Eisen, 2161 (1910).
4. Bredig, M., Franck, H. H., and Füldner, H., *Elecktrochem.*, Bd. **38,** 158 (1932).
5. Bredig, M., Franck, H. H., and Füldner, H., *Elektrochem.*, Bd. **39,** 959 (1933).
6. Carnot, A., and Rcihards, A., *Compt. Rend.*, **97,** 320 (1883).
7. Eisenberger, S., Lehrman, A., and Turner, W. D., *Chem. Rev.*, **26,** 257–296 (1940).
8. Ferguson, J. C., and Merwin, H. E., *Am. Jour. Sci.*, **48,** 48 (1919).
9. Ferguson, J. C., and Merwin, H. E., *Am. Jour. Sci.*, **48,** 165 (1919).
10. Frondel, Clifford, *Am. Mineral.*, **26,** 145–152 (1941).
11. Gruner, J. W., and McConnell, D., *Zeits. Krist.* (A), **97,** 208 (1937).
12. Hendricks, S. B., Jefferson, M. W., and Mosley, V. M., *Zeits. Krist.*, **81,** 352 (1932).
13. Hilgenstock, G., Stahl und Eisen, 498 (1881).
14. Hilgenstock, G., Stahl und Eisen, 557 (1887).
15. Hill, W. L., Hendricks, S. B., Jefferson, M. E., and Reynolds, D. S., *Ind. & Eng. Chem.*, **29,** 1299 (1937).
16. Körber, F., and Trömel, G., *Zeits. Elektrochem.*, Bd. **38,** 589 (1932).
17. Körber, F., and Trömel, G., *Arch. Eisenhüttenwesen*, **1,** 7 (1933).
18. Kroll, V. A., *Jour. Iron & Steel Inst.*, **84,** 126 (1911).
19. McConnell, D., *Am. Mineral.*, **22,** 997 (1937).
20. McConnell, D., *Am. Mineral.*, **23,** 1 (1938).
21. McConnell, D., *Am. Jour. Sci.*, **36,** 296 (1938).
22. Marshall, H. L., Reynolds, D. S., Jacob, K. D., and Rader, L. F. Jr., *Ind. & Eng. Chem.*, **27,** 205–209 (1935).
23. Nagelschmidt, Gunther, *Jour. Chem. Soc.*, 865 (**1937**).
24. Nielsen, O. *Ferrum*, **19,** 97 (1913).
25. Rankin, G. A., and Wright, F. E., *Am. Jour. Sci.*, **39,** 5 (1915).
26. Reynolds, D. S., Jacob, K. D., Marshall, H. L., and Rader, L. F. Jr., *Ind. & Eng. Chem.*, **27,** 87–91 (1935).
27. Schleede, A., Schmidt, W., and Kindt, H., *Zeits. Electrochem.*, Bd. **38,** 633 (1932).
28. Schneiderhöhn, H., *Mitt. Kais.-Wilh.-Inst. Eisenforschg.*, **10,** 213 (1928).
29. Schneiderhöhn, H., *Mitt. Kais.-Wilh.-Inst. Eisenforschg.*, **13,** 109 (1931).
30. Scott, A., and McArthur, D. N., *Jour. West Scotland Iron & Steel Inst.*, **29,** 79 (1922).
31. Stead, J. E., and Risdale, C. R., *Jour. Chem. Soc.*, **51,** 601 (1887).
32. Trömel, Gerhard, *Mitt. Kais.-Wilh.-Inst. Eisenforschg.*, **14,** 25–34 (1932). (With an appended optical description by Schneiderhöhn, p. 34–35.)
33. Trömel, Gerhard, *Zeits. Physikal. Chem.*, *A*, **158,** 422 (1932).

SOME NEW DATA ON THORTVEITITE

JOHN PUTNAM MARBLE, *U. S. National Museum*
AND
JEWELL J. GLASS, *U. S. Geological Survey.**

The rare mineral thortveitite, chiefly of interest as the only available source of scandium in quantity, was first described by J. Schetelig, and has also been studied by A. Lacroix. The data so far presented by both these workers are adequately covered by the former.[1] The crystal structure has been studied by F. Zachariasen.[2] A description of the original locality in Norway, and a discussion of the paragenesis of the mineral has been published by H. Bjørlykke.[3]

Recently the original dyke has been re-opened and a considerable quantity of fresh clean thortveitite has been mined for scientific purposes. Specimens have been added to the collections of the Norges Tekniske Høiskole at Trondhjem, Norway, and the U. S. National Museum, but the greater part of the material is being employed in an investigation of the atomic weight of scandium. As no mineralogical studies have appeared during nearly 20 years, it was thought worth while to investigate this new supply, and briefly report on it, particularly as slight differences from previous work are shown.

The exact source of the material is the dyke described by Bjørlykke as "85 Eptevann 2" on p. 237 of ref. 4. It is situated on the farm Eptevann, Iveland District, about 50 km. N. of Kristiansand S, Southern Norway, 7° 51′ E. Long., 58° 27′ N. Lat.[4]

The mineral was mined by Olav Landsverk of Iveland, and carefully separated from other minerals by Dr. Harald Bjørlykke of the Tekniske Høiskole, Trondhjem. We are deeply indebted to Dr. Bjørlykke for his kindness in making all the arrangements for the supply of material, as well as for the separations, and for much information. The optical and mineralogic studies were made by one of us (J. J. G.) and the chemical analysis by the other (J. P. M.).

Several clean crystal fragments were taken, one being used for optical studies, and portions of four others ground for analysis.

Optical and allied properties were determined on an incomplete section of a grayish-green prismatic crystal measuring 2.5×1.5×1.5 cm. H.

---

* Published by the permission of the Director, U. S. Geological Survey, Department of the Interior, Washington, D. C.

[1] Brøgger, W., Vogt, Th., and Schetelig, J., Die Mineralien der südnorvegischen Granit-Pegmatitgänge. II. Silikate der seltenen Erden (Y-Reihe und Ce-Reihe): *Videnskapsselskapets Skrifter*. I. *Mat.-naturv.* Kl., 1922, No. 1, 51–87, Oslo (**1922**).

[2] Zachariasen, F., *Zeits. Krist.*, **73**, 1 (1930).

[3] Bjørlykke, H., *Norsk Geol. Tids.*, **14**, 211–310 (1934).

[4] Bjørlykke, H., Private communication.

=6–7. G.=3.58. Optically negative, 2V large, calculated 60°–65°. Dispersion distinct, $r>v$, apparently crossed in some grains. Straight cleavage edges are rarely observed. Polysynthetic twinning is distinct but infrequent. Extinction against twinning lamellae, 10°.

The indices of refraction (Table 1) were determined by the immersion method in white light.

TABLE 1. INDICES OF REFRACTION

	α	β	γ	B
	1.752	1.790	1.802	0.050
	1.751	1.789	1.803	0.052
	1.750	1.788	1.803	0.053
	1.751	1.789	1.803	0.052
Average	1.751	1.789	1.803	0.052
By Schetelig[5]	1.756 (−)2V=66°	1.793	1.809	0.053
By Lacroix[6]	1.750 (−)2V=60°–70°		1.802	0.052

It will be noted that our indices are consistently about 0.005 lower than those reported by Schetelig, but agree with those obtained by Lacroix on material from Madagascar.

The analysis gave the following results:

TABLE 2. THORTVEITITE FROM EPTEVANN, NORWAY
J. P. Marble, analyst

SiO_2	45.79%	
CaO	0.24	
MgO	0.17	
MnO	0.53	
ThO_2	0.09	
Sc_2O_3	34.32	
La_2O_3, etc.	1.48	
Y_2O_3. etc.	9.52	
Fe_2O_3	2.95	
Al_2O_3	4.95	
TiO_2	< 0.01	
U_3O_8	0.00	
Pb	0.00	
ZrO_2	0.00	
H_2O (−110°)	0.07	
H_2O (+110°)	0.00	
Total	100.11%	Density (25°/4°)=3.58

---

[5] Schetelig, J., *Norsk. Geol. Tids.*, **6**, 233 (1922).

[6] Lacroix, A., *Comptes Rendus*, **171**, 421 (1920).

All the above figures are the mean of at least two closely agreeing determinations.

A few notes on the analysis may be made. The mineral is very refractory, requiring at least three prolonged fusions with sodium carbonate for decomposition. The resulting large excess of sodium salts interferes with the separations in the rare-earth group. For these determinations, the mineral was repeatedly evaporated with hydrofluoric acid to remove silica, and the insoluble fluorides dissolved by evaporation with nitric acid. Repeated precipitation of the rare-earth group with oxalic acid in a faintly acid solution free from ammonium salts left all other ions in solution. The oxalates were reconverted to nitrates, and after removal of thorium as peroxynitrate, to fluorides. Scandium was removed by solution as the double acid ammonium fluoride in slightly warm acid ammonium fluoride solution, following a suggestion by Noyes and Bray.[7] This seems to give quantitative results. Three experiments gave 34.71, 34.12, 34.13 per cent Sc_2O_3. The lanthanum group oxides as reported, are those whose double potassium sulfates are insoluble. The test is not delicate, and their presence is doubtful. They have not been previously reported in this mineral. Both groups of rare-earth oxides were pale buff in color. The small amount of ThO_2 found was checked by a rough Geiger-counter test by Dr. Wm. D. Urry of the Geophysical Laboratory of the Carnegie Institution of Washington. He estimated the ThO_2 content as "1/20 to 1/10 of 1 per cent."[8] Lead and uranium could not be detected analytically. A trace of lead must be present as the result of radioactive decay of thorium, but this is estimated at about 0.001 per cent, or less than 0.005 mg. in the size of the samples used. The H_2O $(-110°)$ is probably moisture adsorbed on the very fine powder. The MnO and Al_2O_3 are higher than reported by Schetelig in his earlier analyses. Our material may be less pure. ZrO_2 has been reported in thortveitite from Madagascar, but we did not succeed in isolating it in our material. There may be traces thereof in the Al_2O_3. A partial analysis in which the rare-earths and thorium were weighed together shows 45.55 per cent of this group. The sum of the separate oxides is 45.41 per cent, so that little of these oxides seems to have been lost.

We thank the Assistant Secretary of the U. S. National Museum for laboratory and other facilities extended to the senior author.

---

[7] Noyes, A., and Bray, W., A System of Qualitative Analysis for the Rare Elements, New York, pp. 221, 446 (**1927**).

[8] Private communication.

THE BAXTER HOLLOW GRANITE CUPOLA*

R. M. Gates,
University of Wisconsin, Madison, Wisconsin.

Abstract

The Baxter Hollow granite is interpreted as an intrusive into the Baraboo (Huronian?) quartzite. Cleavelandite dike apophyses in the advancing roof are brecciated and modified to a very unique biotite-bearing type of xenolith.

General Statement

The Baraboo quartzite is a pre-Cambrian inlier in the Paleozoic strata of south central Wisconsin, occurring as a well known "canoe shaped" fold (1). The quartzite is probably Huronian in age. On the south margin of the fold, where Otter Creek flows through Baxter Hollow, a granite body is exposed below the quartzite. The granite is shown here to be intrusive into this quartzite. Since this is a controversial question to which attention has been given in the literature, this point is discussed in detail. The granite is regarded as a cupola subsidiary to a large batholithic mass which extends through central Wisconsin. The purpose here is (a) to discuss the intrusive relationship, and (b) to trace as far as possible the unusual rock types encountered.

History of the Problem

In 1904 S. Weidman (2) first described these igneous rocks as a granite "varying in color from grayish to reddish and (which) consists of feldspar, quartz, and a small amount of dark mineral." He considered the rock as part of the pre-Baraboo quartzite basement.

Later Alden (3) quoted Steidtman to the effect that the granite was intrusive into the quartzite. Steidtman had expressed this view in a letter to F. T. Thwaites but withdrew his conclusion.

Stark (4), in 1932, concluded that the granite was basal to the quartzite. He described a "dark green phase" of the granite, which due to lack of any intrusive relationship, he attributed to magmatic differentiation.

Field (5) concluded (a) that the granite was basal to the quartzite and that the quartz-tourmaline veins found in the quartzite did not come from the granite, and (b) that "the granite of the area, other than the medium-grained pinkish type, are results of the assimilation of the basic material by the granite." A very small, isolated, outcrop of a basic rock was found in this area by Field—it is still unexplained.

---

* This work was supported in part by a grant from the Wisconsin Alumni Research Foundation.

Regional Relationship of the Cupola

Throughout central Wisconsin granite is exposed which, though varied lithologically, is interpreted by Emmons (6) as apparent phases of one batholithic mass. The batholith is thought to extend north at least to Wausau, east to Shawano, and south-east to New London. The granite at Montello, because of its granophyric nature, is regarded as part of this same body. Emmons regards the pegmatite dikes at Waterloo and the Baxter Hollow body as still farther southward expressions of this same batholithic mass. That is, only the roof of the batholith is exposed and the contact with the overlying rocks is, in this part of Wisconsin, nearly horizontal.

Granophyric roof rock material is quarried at Montello and at Red Granite. The rock is medium to fine grained and is composed essentially of a myrmekitic intergrowth of quartz and feldspar. An overlying rhyolite is found nearby at Endeavor. Elsewhere in the region the granite shows variations suggestive of assimilation and hybridization. This effect ranges from migmatites and metagabbros through diorite and rapakivi granite to biotite granite and even syenite. Several phases of this broad problem are now being studied in detail by others and will be reported on in due time. The present study is to be regarded as one of such a series.

The Baxter Hollow cupola is regarded as one of the upward extensions of the underlying magmatic body referred to above. Rhyolites and associated rocks, in general, underly the quartzite. Near Denzer, about three miles west of Baxter Hollow, is a water laid tuff. The Merrimac rhyolite flow is about five miles to the east. Only at Baxter Hollow, of the Baraboo district, is granite found. The shape or extent of the granite body is concealed by the Paleozoic strata, but its direct connection with a parent body is suggested by the marked indications of hydrothermal activity on the upper side.

The proximity of an intrusive igneous body is also suggested by veinlets which cut the quartzite. Small veins of quartz and specular hematite are well distributed in the Hollow and have been reported at the Lower Narrows and elsewhere. Veins of quartz and tourmaline occur in both Baxter Hollow and Pine Hollow (three miles apart). Sericite is found in the quartzite near the granite at Baxter Hollow and has been reported elsewhere in the district. At Ableman's, pockets of sericite in the quartzite appear to have been filled by ground water which has gathered the sericite from the quartzite above. A diorite outcrops near Denzer.

Age Relationships

Major interest doubtless centers on the age relationships of the granite and the quartzite. Both field observations and laboratory study support the conclusion that the granite is younger than the quartzite. The following observations are chosen as pertinent:

1. There is a notable shear zone below the quartzite and above the granite. This shear zone differs from the rest of the granitic rocks in being mainly gray in color, rather than the prevailing red or pink. At no point was the contact seen between this gray sheared rock and the quartzite, though the quartzite may be traced to a point within 5 or 6 feet of it.

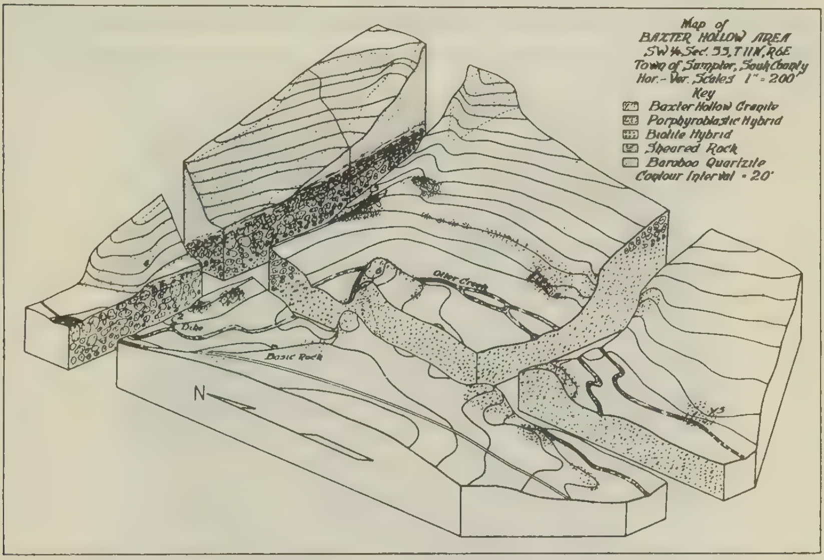

FIG. 1.

Although the evidence seems good that the shear zone is beneath and parallel to the quartzite, yet another possibility was considered and rejected; namely, that it is a vertical shear zone cutting the quartzite and the granite. Fracture cleavage in the shear zone would satisfy either hypothesis. Selected as a deciding factor is the distribution of sheared rock outcrops as shown in the accompanying map (Fig. 1) and also as mapped by Field. They lie in a plane which is parallel to the bedding planes of the quartzite. Confusion is introduced by the fact that all but one of these outcrops lie in a nearly vertical plane which strikes about east-west and is almost parallel to the mapped cliff faces.

This shear zone hides the immediate relationship between the granite and the quartzite. The competent member serves as a buttress against which shearing is developed—a type of occurrence frequently recorded in the literature. In fact, on the other side of the Baraboo syncline, at the

Lower Narrows where the quartzite with its basal conglomerate rests on rhyolite, the shearing is concentrated in a relatively narrow zone near the quartzite. At a comparatively short distance from the quartzite the rhyolite is massive. It is fair to assume then that both shear zones are younger than the quartzite and represent the shearing of whatever rock underlay the quartzite. There remains to examine now the relative ages of the granite and the sheared rock.

2. Although the main granitic mass is composed of angular blocks 'floating' in granite, there is a uniformity to the whole, apparently to be attributed to the reaction of the granite with its stoped material. This is discussed later. One is not conscious, however, of more than an occasional dike of granite cutting the main body. But in the shear zone, especially at one point (point 1 on map) small, but definite reticulating apophyses of red granite cut the sheared rock. It seems immaterial whether these apophyses are frozen granitic liquid or hydrothermal solutions from the granite—the conclusion that the granite is younger still holds. It should be added that where the apophyses cut the sheared rock, the cleavage is largely, but not entirely, destroyed—presumably the rock is made over in part. Since an apophyse of pre-quartzite age would not necessarily be destroyed on shearing, then the field facts, though strongly suggestive, are not definite proof of a younger granite.

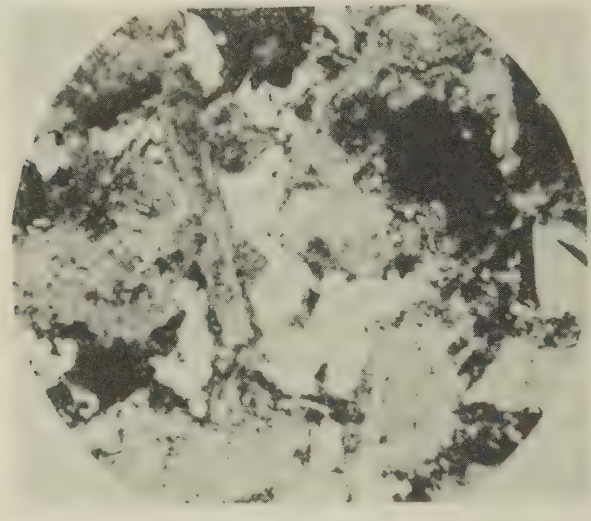

FIG. 2. Photomicrograph (×30, crossed nicols) of cleavelandite dike rock showing tabular feldspars highly sericitized and poikilitic quartz.

3. Under the microscope there is evident a definite relationship between the amount of sericitization in the rocks underlying the quartzite

and the proximity to the quartzite. Remote from the quartzite the feldspars in the granite apophyses are fresh enough that their twinning is observed, extinction may be measured, and the feldspar may be identified by any of the standard methods. Near, and in the shear zone on the other hand, the feldspars are thoroughly sericitized—commonly so much so that only their outline, sericite pseudomorphous after feldspar, remains to identify their former presence (Fig. 2, point 2 on map). This observation is sufficiently consistent to indicate a relationship between the granite and the shear zone. If such a relationship is true—that late hydrothermal solutions from the granite have altered the sheared rocks—then of course the granite is younger than the quartzite. The only alternative view is that the shear zone has been a locus of solution channels from which solutions emanated. The first explanation is chosen as much the simpler and more plausible. The shear zone shows no lit-par-lit injection.

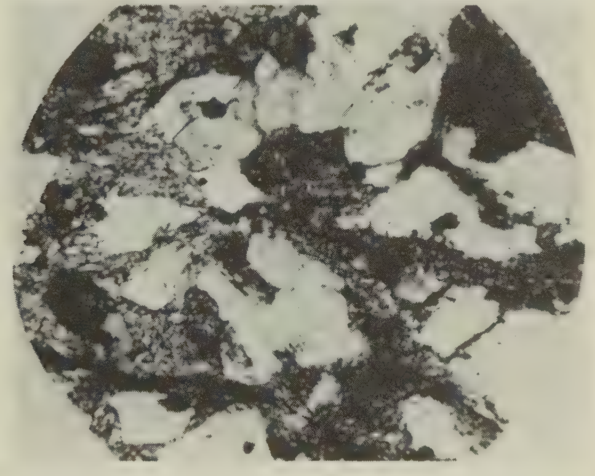

Fig. 3. Photomicrograph (×80, crossed nicols) of sheared rock. Notice quartz poikilitically enclosing sericite—all quartz in photomicrograph has a common orientation.

4. Rock from the shear zone, in general, shows the customary sheen on its cleavage surface in hand specimen and shows good alignment of mica in thin section, though this is often obscured by later alterations of a sericitic nature. Most significant is the poikilitic quartz which characterizes all specimens examined from the shear zone. There is no tendency for the mica to bend around these quartz crystals (Fig. 3, point 3 on map). It is a fair conclusion that much of the sericite and a great deal of the quartz postdates the shearing.

5. Thin sections of the quartzite, near but above the shear zone, show shattering and sericitization; the sericite being distributed interstitially in brecciated portions of the rock (Fig. 4, point 4 on map). In general however, there is little evidence of actual igneous material in the quartzite.

6. A general gradation in three respects exists in the hybrid rocks below the quartzite. Exceptions to this gradation have been found, but are apparently quantitatively unimportant. These gradations are in respect to the degree of sericitzation, the number of porphyroblasts, and the amount of poikilitic quartz. The increase in sericitization approaching the quartzite is described in paragraph 3 above.

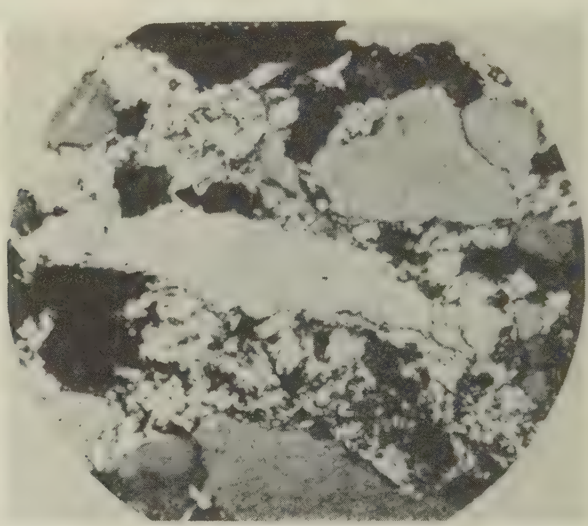

Fig. 4. Photomicrograph (×95, crossed nicols) of sericite in quartzite above shear zone.

If the quartzite with its present attitude (strike E-W, dip 12° N) were extended toward the south, it can readily be seen that the rocks at the south end of the Hollow are farthest below the quartzite, and those at the north end are nearest the quartzite. The gradations then are from the rocks at the south end of the Hollow to those at the north end.

The gradation in respect to the number of porphyroblasts can best be observed in the hand specimen. The rocks at the south end of the Hollow are characterized by an abundance of porphyroblasts and are called the porphyroblastic hybrid. The porphyroblasts decrease rapidly in number toward the middle of the Hollow and are apparently non-existent at the north end. Thus, the rocks grade from a porphyroblastic hybrid remote from the quartzite to an even-grained hybrid (later described as biotite hybrid) adjacent to the quartzite.

The gradation in respect to the type of quartz was observed in numerous thin sections of rocks throughout the Hollow. Again exceptions have been found, but the generalization is true. The quartz varies from small grains in random orientation in the rocks farthest from the quartzite (Fig. 5, point 5 on map) to large patches with a common orientation, poikilitically including feldspar crystals in rocks nearest the quartzite (Fig. 3 or 6). Poikilitic quartz is especially abundant in the shear zone adjacent to the quartzite. Therefore, there is an apparent increase in size of the quartz grains (or in poikilitic quartz) as the quartzite is approached.

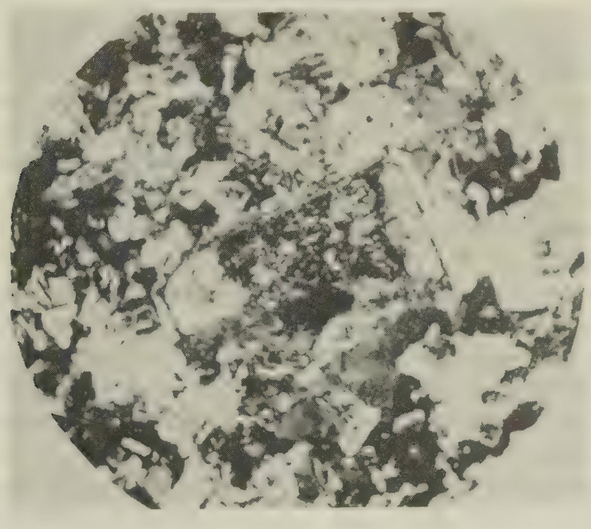

Fig. 5. Photomicrograph (×30, crossed nicols), of porphyroblastic hybrid at south end of Hollow. Notice zones of sericite on porphyroblast.

These several observations fall into a logical sequence of events in the following interpretation. Folding and intrusion progressed simultaneously, as is usually true, though folding was not at all severe at this locality. A shear zone quite apparently developed before the intrusion reached the quartzite, or at least before the last effects of the intrusion reached the quartzite. As the granite encountered the quartzite base, folding continued, whereby, to a considerable extent, the active shear zone served as a seal to the granitic juices. The word 'juices' seems especially appropriate here since there is comparatively little evidence of real granite liquid and an overwhelming amount of sericitization, indicating much hydrothermal activity. Possibly some of the stoped blocks in which the exposed granite abounds, are quartzite—that is mere speculation. It will be suggested below that they are, in part at least, arkose or rhyolite. In any case, the field facts suggest that the ability of the granite to stope was virtually suspended at this stage, otherwise more clean red granite and less hybrid would be expected.

This interpretation is offered to account for the following facts: (1) The extensive sericitization and development of poikilitic quartz near the quartzite; (2) The limited penetration of the quartzite by any part of the granite; (3) The cleavelandite dikes discussed below; and (4) The varied course of hybridization to be discussed next.

Rock Types Within the 'Granite'

The rock types in the Hollow have a special interest, in that they illustrate the chemical effect of the intrusion on a host of stoped blocks, and some of them suggest the effect on the intrusion of the same stoped blocks. The mutual effect has gone so far that the original rock types of the intrusive or the wall rocks are not available for examination.

The most 'normal' intrusive material is granophyric; the least modified of the wall rock type is apparently an arkose or coarse tuff. All rocks below the quartzite show more or less sericitization and usually much more than the average granite. Except for narrow zones on feldspars of a few of the rocks (Fig. 5), there is little fresh feldspar to be found. The sericitization appears in two dominant aspects—very fine, masking alterations, and a coarser development in which the individual flakes are easily seen under low power. This coarser type commonly, but not always, occurs as a reticulating network of microscopic veinlets.

Before discussing further generalities, let us review the rock types in detail. The main rock types in the cupola, which in general grade into one another, are: (1) the Baxter Hollow Granite (normal red granite), (2) biotite hybrid, (3) pegmatite hybrid, (4) porphyroblastic hybrid, (5) arkose, (6) sheared rock, and (7) the cleavelandite dike rock. The accompanying map shows the areal distribution of these rock types as far as generalization seems possible. The only other rock type of importance found in the Hollow—the Baraboo Quartzite—has been repeatedly described in detail (1) and needs no further description here.

The compositions of the rock types, as determined by Rosiwal analysis, are tabulated in Table 1. The albite-anorthite ratio of the plagioclases for all rock types was determined in two ways for each grain selected for study—(1) from the Fedorov migration curves (7), and (2) by extinction angles in the zone at right angles to (010), measured from (010) to alpha, using the curve of Michel-Levy. All data were obtained from grains oriented on the five axis Universal Stage. The results check within the accuracy of the extinction angle curve and Fedorov's curves.

The Baxter Hollow Granite. The 'normal' granite is red to light pink,

TABLE 1

Rock Type	% Feldspar	% Quartz	% Biotite or Chlorite
(1) Granite	66.2	29.1	4.6
(2) Porphyroblastic Hybrid	71.2	25.5	3.2
(3) Pegmatite Hybrid	68.9	22.2	8.9
(4) 'Arkose'	66.0	34.0	—

very fine grained, and contains few dark minerals. Only some of the pegmatoid veins approach the coarseness of a normal granite. The feldspars are sericitized and have a reddish tinge. Much of the plagioclase is more sericitized than the orthoclase. The plagioclase generally shows albite twinning and has a composition of $Ab_{95}An_5$. Orthoclase and plagioclase are found in the ratio of about 2:1. Minor amounts of microcline and microcline perthite are also present. Biotite is the only important dark mineral and is green, in flakes, and in places is altered to sericite or chlorite.

The Biotite Hybrid (see matrix of porphyroblastic hybrid in Fig. 5). This hybrid is a gray-green rock which varies considerably throughout the Hollow in texture and percentage of dark minerals (biotite and chlorite). Textures range from a fine grained 'arkosic' type to a pegmatoid poikilitic one. The feldspars vary from small, irregular, slightly sericitized grains to heavily sericitized, long tabular or lath shaped crystals. The quartz in the finest grained rocks generally occurs as small individual grains with random orientation. In the coarser textured rocks the quartz grains are larger and poikilitic, that is, patches of quartz have a common orientation. The biotite (generally partly altered to chlorite) varies from small rectangular specks to long slender blades cutting across quartz, feldspar, and other blades of biotite. The type of feldspar is hard to determine because of sericitic alteration, but there is an apparent increase in the amount of plagioclase in the coarser textured hybrid. In the coarsest grained biotite hybrid the feldspar is dominantly plagioclase. The composition of the plagioclase in these hybrids varies from $Ab_{100}An_0$ to $Ab_{94}An_6$. Near the quartzite the biotite hybrid appears to be 'soaked' with granite; red feldspar grains stipple the rock. In thin sections of this 'soaked' hybrid the form of feldspar remains, but the mineral is sericite poikilitically included by quartz.

Pegmatite Hybrid (Fig. 6, point 6 on map). This pegmatite hybrid is undoubtedly the most interesting and baffling rock in the Hollow, both petrographically and genetically. Its peculiar appearance in the field first prompted Dr. Emmons and later the writer to undertake a restudy of the area in an attempt to learn its origin. It is the coarsest grained biotite hybrid and is characterized in thin section by long laths of feldspar, poikilitic quartz, and long blades of biotite; and, in the field by a peculiar fracure. It is called pegmatite hybrid to distinguish it from the 'normal' biotite hybrid since its origin is thought to be somewhat different. In order to facilitate the recognition of this rock in the field, it may be described as pale greenish-brown in color and breaking with a rough surface composed of irregularly oriented plane facets, rather than the consistently rough surface of the ordinary granite or inclusion. Both features are to be attributed to cleavage within the biotite flakes.

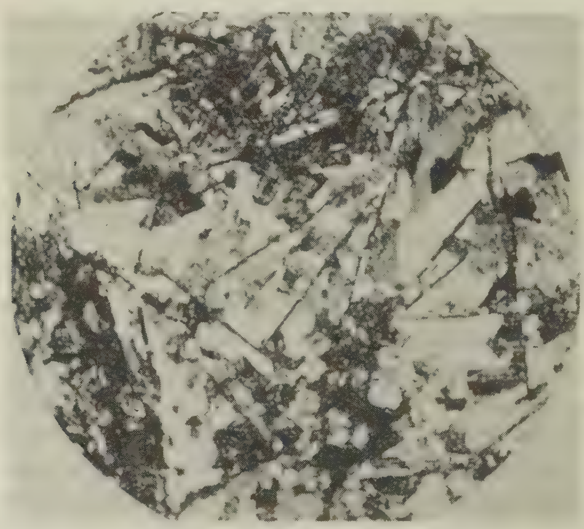

FIG. 6. Photomicrograph (×30, crossed nicols) of pegmatite hybrid showing poikilitic quartz and long blades of biotite.

A few facts concerning the occurrence of the pegmatite hybrid may well be given here. This rock occurs almost exclusively as apparent inclusions in what is now red granite or porphyroblastic hybrid, or what probably were the main solution channels. It must not be forgotten that the 'normal' biotite hybrid which grades into the pegmatite hybrid also occurs there. Sharp contacts can be found between the pegmatite hybrid and nearly all other rocks in the Hollow. Particularly numerous are sharp contacts with the red granite. The only place where the pegmatite hybrid could not be found was directly below the quartzite outcrops at the north end of the Hollow. This will be discussed later.

The Porphyroblastic Hybrid (Fig. 5). This rock varies from a gray hybrid (essentially a fine to medium grained biotite hybrid) with few porphyroblasts to a light tan hybrid with abundant porphyroblasts. The biotite hybrid occurs here as inclusions cemented by the porphyroblastic hybrid. The porphyroblasts are almost exclusively plagioclase and they range in size from microscopic to one-half inch in diameter. They are generally either euhedral and evenly sericitized or are rounded and have zones of sericite (Fig. 5). The evenly sericitized euhedral porphyroblasts usually have a composition of $Ab_{95}An_5$, while those with clear outer zones have compositions of $Ab_{85}An_{15}$. Porphyroblasts with compositions between $Ab_{95}An_5$ and $Ab_{85}An_{15}$ are also present. Occasionally the plagioclase is zoned—the core being $Ab_{95}An_5$ and the outer zone being $Ab_{85}An_{15}$. The matrix of quartz, feldspar, and biotite enclosing the porphyroblasts frequently exhibits evidence of crushing. Biotite and chlorite occur both as flakes and thin blades. Black biotite flakes are conspicuous in the hand specimen in the crushed zones between inclusions of biotite hybrid in the porphyroblastic hybrid.

The 'Arkose.' The 'arkose' is a fine grained rock composed of quartz and feldspar in a mosaic pattern. The 'arkose' is generally found intimately intermingled with the red granite in the more prominent dikes or apophyses. It does, however, have a sharp contact with the granite in all cases observed. It is much finer grained than the granite, but has essentially the same composition except for the absence of biotite. The feldspar is largely orthoclase, about one-third being plagioclase. The feldspar is reddish colored and only slightly sericitized as compared with the other rocks in the area. The quartz occurs as small rounded grains in random orientation.

The Sheared Rock (Fig. 3). The sheared rocks as shown on the map occur in a zone 10 to 20 feet thick directly below the quartzite. The minerals in the sheared rocks are quartz, feldspar, sericite, and biotite partly altered to chlorite and magnetite. The quartz generally poikilitically encloses masses of sericite and feldspar. The feldspar is almost completely altered to sericite. The sheared rock nearest the quartzite is quite schistose, becoming less and less so as it grades down into the granite and biotite hybrid.

The Cleavelandite Dike Rock (Fig. 2, for picture of dikes see reference (6) Figs. 1 and 2). The feldspar in the dike rock has a cleavelandite or tabular texture in the hand specimen, but it is difficult to see that texture in thin section. The photomicrograph does show one lath-shaped crystal completely altered to sericite. The quartz is poikilitic and the feldspar is almost completely altered to sericite. The texture of the dike rock is quite similar to that of the pegmatite hybrid except for the blades of biotite.

GENESIS OF THE ROCK TYPES WITHIN THE GRANITE

As previously stated, the map and cross sections show the areal distribution of the rocks as far as possible. It is evident that the massive biotite hybrid, penetrated by granitic stringers, veins, and dikes, is nearest the quartzite and the porphyroblastic hybrid, with many small biotite hybrid inclusions, is farthest away. Since the hybridization process was progressive, many stages in the development were frozen; hence the varieties recorded. There is an apparent gradation from any one type to any other —particularly from the 'arkose' to the biotite hybrid to the pegmatite hybrid—if specimens are selected with this purpose in mind. Therefore, virtually any interpretation which depends on such a gradation may be 'proved' by specimens. Similarly, rather sharp boundaries may be found between almost any two rock types, which in turn may be used to prove a lack of gradation.

The pegmatite hybrid apparently is the key to the origin of the Baxter Hollow rock types, and with that in mind an attempt will be made to trace the development of this unusual rock. A general history of the Hollow as I interpret it is this: Quartzite, presumably underlain by arkose or rhyolitic tuff, was folded and intruded. Into the initial fractures flowed the most mobile granitic juices, permeating and altering the wall rock, and then froze to form dikes like those mentioned above (see cleavelandite dikes). Continued folding and intrusion brecciated the arkose and the early formed dikes further and subjected both to the effects of the granitic juices. The usual metamorphic processes—recrystallization, growth, and development of biotite—altered the arkose to the normal biotite hybrid and the dike rock, essentially a cognate inclusion, to the present pegmatite hybrid. Thus the gradation getween the arkose and the pegmatite hybrid is the usual one between wall rock and the granitizing juices, except that here the initial intruding juices were solidified, later brecciated, and then subjected to the same metamorphism as the wall rock. The original texture of the dike rock probably accounts for the blade-like form of the biotite in the pegmatite hybrid. In this way the igneous nature of the quartz and feldspar, and the metamorphic appearance of the biotite is logically explained.

There is an apparent increase in sericitization and poikilitic quartz development as the quartzite is approached. This increase suggests a greater concentration of solutions near the quartzite, a condition which requires explanation. Although other explanations may be suggested, the following one appears to satisfy the field facts as outlined. The greater aggregation of inclusions is near the quartzite, which is also where shearing is greatest. Movement at this horizon would create an area of low pressure to which the more mobile constituents of the intrusive should migrate, hence the greater amount of solution action. It is entirely reasonable that, more remote from the quartzite, the present prophyroblastic hybrid was earlier a different type of rock, more nearly similar to the normal biotite hybrid which is immediately below the quartzite—but since altered to its present state by deeper burial in the granite magma.

The shear zone below the granite is regarded as an effective barrier to granitic juices. Some escaped into the quartzite as indicated above, but in general, solutions were trapped here. The effectiveness of this trap was enhanced by movement during intrusion. Solution channels through the shear zone were closed almost as fast as they were formed. The type of solution channel which prevailed in this general area is believed to be typified by the dike-like bodies mentioned above (see ref. 6, Figs. 1 and 2). This entire explanation, if correct, would involve a saturation of the shear zone rocks. This is in complete agreement with the facts in that, as pointed out previously, the sheared rocks are well recrystallized. In the field the sheared effect is very evident a few feet away and again by the use of a hammer. But the usual sheen which characterizes a schist is not as expected.

The fine grained red Baxter Hollow granite is thought to have been introduced very late in the history of the cupola along new fractures which followed the old solution channels and which tapped the original magma chamber.

Acknowledgments

The writer gratefully acknowledges the continual assistance of Dr. R. C. Emmons in the laboratory, in the field, and in the writing of the paper. The cupola-like nature of the granite body and its relation to the quartzite were first recognized by Dr. Emmons.

The writer is also indebted to Ted Townsend and C. W. Gates for assistance in mapping the area. Thanks are also due Drs. W. H. Twenhofel, H. E. McKinstry, and S. A. Tyler for criticizing the paper.

References

1. Irving, R. D., The Baraboo quartzite ranges; *Geol. Wis.*, **2,** 504–519 (1877).
2. Weidman, Samuel, The Baraboo iron-bearing district: *Wis. Geol. and Nat. History Survey, Bull.* **13,** Econ. Series No. 8 (1904).
3. Alden, W. C., *United States Geol. Survey., Prof. Paper* **108,** The quaternary geology of southeastern Wisconsin (1918).
4. Stark, J. T., Igneous rocks in the Baraboo district, Wisconsin: *Jour. Geol.*, **40,** No. 2 (1932).
5. Field, George William, The Baxter Hollow granite, an unpublished thesis at Wisconsin (1935).
6. Emmons, R. C., The contribution of differential pressures to magmatic differentiation: *Am. Jour. Sci.*, **238,** 1–21 (1940).
7. Emmons, R. C., Plagioclase determination by the modified universal stage: *Am. Mineral.*, **19,** 237 (1934).

X-RAY EVIDENCE OF THE EXISTENCE OF THE MINERAL DIGENITE, Cu_9S_5

NEWTON W. BUERGER,*
Queen's University, Kingston, Ontario.

ABSTRACT

X-ray studies of the system Cu_2S-CuS have shown the existence of the compound Cu_9S_5 as a separate phase. The diffraction pattern produced by this intermediate compound corresponds with that obtained from a type specimen of digenite, a mineral apparently among *Dana's* discredited species. There is no room for doubt now that the mineral exists, and is indeed the familiar "isometric chalcocite." This is obvious from a comparison of the diffraction pattern of digenite with those obtained by Kerr on three samples of "isometric chalcocite" from Kennecott, Alaska, and by Kurz on the same material; patterns are identical. Since digenite is in fact a rather common mineral occurring with chalcocite and other copper ore minerals, it must be re-established as a species.

In order to investigate the solid phases of the system of Cu_2S-CuS (1), a series of homogenous samples were prepared for *x*-ray study having compositions grading between Cu_2S and CuS. These samples contained the following per cent of CuS by weight: 5, 8, 9, 10, 11, 13, 14, 15, 20, 30, 40, 50, 60, 70, and 80.

Appropriate end-member materials for these mixtures are selected as follows: For the chalcocite end-member, it was known that the Bristol, Connecticut, chalcocite yields an ideal Cu_2S analysis (2, p. 508). Accordingly, a large single crystal of this material was crushed and the fragments examined by several means, including examination of polished sections with the aid of reflected polarized light. All such tests confirmed the preliminary impression that this chalcocite was pure, homogeneous material and would make an ideal Cu_2S end-member. For the CuS end-member, it was at first thought possible to use pure natural crystals. The covellite from the Leonard Mine, Butte, Montana, was selected as the purest material available for this purpose. It was found, however, that it was impossible to hand pick even a small amount of this mineral and obtain a product which was uncontaminated by chalcocite, bornite, and other associated minerals. However, it fortunately proved possible to obtain synthetic CuS of high chemical purity. *X*-ray powder photographs proved this material to be structurally identical with pure natural covellite. This was an extremely important point in facilitating the experimental work, for it provided an easily obtained, pure covellite end-member.

---

* On leave of absence from Queen's University having been called to active duty as Lieutenant in the United States Naval Reserve. Now on the Staff of the United States Naval Academy, Postgraduate School, Annapolis, Maryland.

The samples of this series of mixtures were annealed and homogenized as powder compacts by a method described elsewhere (1, p. 23). Powder photographs of the entire series including the end-members were then made, using a Debye type powder camera and filtered copper radiation supplied from a hot cathode *x*-ray tube. A careful analysis of the powder photographs of this series indicated that they were composites of two of three patterns, namely the two end-members, and another unique pattern which occurred in pure form at a composition about 13 per cent CuS by weight. The field from pure CuS to this composition gave powder photographs which formed a graduated series of mechanical mixtures from CuS to the 13 per cent pattern, the lines of one component decreasing in intensity and finally disappearing as the other is approached. The field from 13 per cent CuS to about 8 per cent CuS gave powder photographs which also formed a graduated series of mechanical mixtures. The solid solution region, from Cu_2S to about 8 per cent CuS, gave the Cu_2S pattern only. It was concluded, therefore, that there were three distinct compounds in this system stable at room temperatures, namely Cu_2S, CuS, and an intermediate compound having a weight composition of 87 per cent Cu_2S, 13 per cent CuS. This compound has an atomic composition of 80 per cent Cu_2S, 20 per cent CuS, and therefore has a formula of $4Cu_2S \cdot CuS$, or Cu_9S_5.

The possibility immediately suggested itself that this hitherto unrecognized compound, Cu_9S_5, might correspond with one or both of the minerals *digenite* (presumably Cu_5S_4) or *carmenite* (presumably Cu_3S_2). It will be recalled that since *Dana* had found visible covellite in carmenite, both of these species have been regarded as discredited. To test the possible identity of the compound Cu_9S_5 with these, powder photographs were made of digenite from Mansfield, Harz, Germany, and of carmenite from the type locality, Carmen Island, Gulf of California, Mexico.

A study of these photographs showed that digenite gave a pattern which was definitely distinct from both Cu_2S and CuS, but which corresponded exactly with the new phase containing 13–14 per cent CuS, i.e., with Cu_9S_5.

Carmenite, however, gave a pattern which was composed of covellite lines, mainly, with some other lines which were probably caused by some other mineral, or minerals.

Digenite, therefore, was established as the third stable mineral (at room temperature) in the system, while carmenite definitely does not belong in the system Cu_2S-CuS.

The data thus obtained seemed to offer certain interesting speculations. Indeed, at this stage in the study, an explanation could be advanced for a point of fact which should always have puzzled economic geologists. In published accounts of chalcocite occurrences one not infrequently finds photographs of polished sections showing mixtures of white orthorhombic chalcocite and "blue isometric chalcocite," intimately associated in a structure which suggests unmixing, or at least contemporaneous growth. If these two minerals are really polymorphous forms of the same composition, it is very difficult to explain this incongruous co-existence, for it would be expected that the unstable isometric form should invert to the stable orthorhombic modification, especially in the presence of an abundance of crystallization nuclei, or "seed crystals" of the orthorhombic form which are present.

Table 1. Comparison of Interplanar Spacings

Index	Cu_9S_5	"Isometric Chalcocite," Kennecott, Alaska	
		Kerr	Kurz
(?)	—	3.93 Å (diffuse)	—
111	3.25 Å	3.22	3.21 Å
200	2.78	2.88	2.78
220 β	2.51	2.41	—
220 α	1.950	1.975	1.96
311	1.665	1.685	1.677
222	1.60	1.516	—
400	1.386	1.445	1.39
133	--	—	—
420	1.315	1.335	1.244
422	1.135	1.140	1.135
511 333	1.070	1.076	1.070
440	.983	.977	.983
531	.943	.938	.940

On the other hand, if "blue chalcocite" is in reality the mineral digenite, a distinct species with not even the composition of chalcocite, but having the composition Cu_9S_5, it is permissible for the two minerals to exist together, and, in view of the similarity of compositions, it is expectable that they *would* exist together and be intimately associated.

Some light is now shed on the seemingly contradictory results of some of the earlier investigators. Barth (3) made powder photographs of chalcocite at 200° C. and obtained an isometric structure, whereas Rahlfs (4) made similar photographs at 170° C. and noted a nonisometric pattern. Rahlfs did, however, get an isometric pattern at 170° C. using material of the composition $Cu_{1.8}S(Cu_9S_5)$. Kurz (5), using orthorhombic chalcocite, observed no inversion to the isometric modification up to 200° C. Barth's

TABLE 2. COMPARISON OF θ VALUES

Line	Indices	$\sum H^2$	1 Cu_9S_5 NWB	2 α-chalcocite Barth	3 "Isometric chalcocite," Jerome, Ariz. Harvard	4 "Isometric chalcocite," Kennecott. Kurz	5 "Isometric chalcocite," Butte, Mont. Kurz	6 "Isometric chalcocite," Khan Mine. Kurz	"Isometric chalcocite," Tsumeb Mine. Kurz
1	111	3	13.9	—	13.9	13.94	13.9	—	13.9
2	200	4	16.1	15.92	16.0	16.04	16.05	16.14	16.01
3	220 β	8	20.9	—	—	20.7	20.63	—	20.83
4	220 α	8	23.2	22.90	23.2	23.15	23.05	23.12	23.16
5	311	11	27.5	27.19	27.5	27.55	27.26	27.69	27.31
6	222	12	28.7	—	—	—	—	—	—
7	400	16	33.7	33.25	33.7	33.54	33.61	33.06	33.51
8	133	19	—	—	—	—	—	—	—
9	420	20	35.8	37.95	—	38.10	38.05	37.98	38.20
10	422 511	24	42.7	42.57	42.9	42.89	42.65	42.83	42.80
11	333	27	46.0	45.57	46.0	45.93	45.96	—	46.11
12	440	32	51.5	51.11	—	51.46	52.21	51.37	50.6
13	531	35	54.7	54.38	—	—	53.79	—	—

results are discussed in another paper (1), but it should be mentioned here that orthorhombic chalcocite does not invert to an isometric form at a high temperature, but rather to a hexagonal modification, while digenite retains its isometric structure at elevated temperatures.

In comparing the various published *x*-ray data on so-called "isometric chalcocite" it is found that in every case the patterns obtained from such material correspond with that obtained from Cu_9S_5, and are not similar in any respect to that of the high temperature form of chalcocite. Table 1 shows the interplanar spacings of Cu_9S_5 compared with those of "isometric chalcocite" from Kennecott, Alaska. It is quite obvious that the materials giving rise to these patterns were the same in each case. In Table 2 a comparison is given between the patterns of Cu_9S_5 and of six so-called "isometric chalcocite" specimens, including the Jerome, Arizona, "fire zone" material.[1] Again there can be no doubt that all of these are identical structures.

In view of this evidence it must be recognized that a mineral having the composition Cu_9S_5 exists, and is in fact the rather common mineral incorrectly called "isometric chalcocite" and "blue chalcocite." It would seem to be highly desirable to reinstate the name *digenite* for this mineral since the powder pattern obtained from a type speciment of digenite from Mansfield, Germany, corresponds with that of Cu_9S_5.

REFERENCES

1. BUERGER, NEWTON, W., The chalcocite problem: *Econ. Geol.* **36,** 19–44 (1941).
2. POSNJAK, EUGENE, ALLEN, E. T., AND MERWIN, H. E., The sulphides of copper: *Econ. Geol.*, **10,** 491–535 (1915); also Table XI, p. 508.
3. BARTH, TOM, Die reguläre Kristallart von Kupferglanz: *Central. Min.*, etc., A (1926), 284–286.
4. RAHLFS, PAUL, Ueber die kubischen Hochtemperaturmodifikationen der Sulphide, Selenide und Telluride des Silbers und des einwertigen Kupfers: *Zeits. phys. Chem.* (B), **31,** 157–194 (1936).
5. KURZ, WOLDEMAR, Chemisch-röntgenographische Untersuchung am "blauen Kupferglanz": *Zeits. Krist.*, **92,** 408–434 (1935).

[1] Dr. Harry Berman of Harvard University kindly supplied the powder photograph of the Jerome material from which the data given in Table 2, column 3, were obtained.

NOTES AND NEWS

AN OCCURRENCE OF ILSEMANNITE

E. D. Goldring,
Saratoga, Wyoming.

Introduction

Ilsemannite, $MoO_3 \cdot SO_3 \cdot 5H_2O$, was first described a number of years ago, and the literature contains numerous references to its occurrence. Despite these facts, it remains one of the lesser-known minerals; few of its physical and chemical properties have been determined. Dana (1) classified it as a molybdenum molybdate, assigning to it the formula, $MoO_2 \cdot 4MoO_3$. Schaller (2) proved it to be a hydrous molybdenum sulfate, a fact later confirmed by Hess (3).

During the course of some investigations conducted early in the year at the fluorspar mine operated by the Western Fluorspar Corporation, in northern Jackson County, Colorado, a blue incrustation, superficially resembling azurite, was noted on the drift walls. The writer was informed that the material had been identified as ilsemannite by the late Professor Wm. E. Ford. More recently, developement work has yielded a muck which, after a few days' exposure on the mine dump, has become ilsemannite-incrusted, although no indication of the mineral was apparent in the freshly mined ore. Because of some unusual features of the occurrence a brief description may be of interest.

Geology of the Occurrence

Workings at the mine referred to above are confined to drifts and stopes on two parallel fault fissure veins, approximately fifty feet apart and dipping nearly vertically. The country rock is a reddish pre-Cambrian granite, changing into a bluish granite in the vicinity of the veins. The vein filling is largely fluorspar mixed with fragmented granite torn from the walls during processes of faulting. Huge granitic "horses" are not uncommon. The granite inclusions are rusty brown in color, and have been partly replaced by fluorite.

While the ilsemannite, and ore which has subsequently become incrusted with it, has been found in various parts of the mine, the most important source has been a zone of disturbance thirty feet in width crossing the veins at an angle of about 25°. This zone is occupied by fault breccia consisting of angular fragments of fluorspar, quartz, and granite, in a matrix which is highly decomposed, and is commonly friable and somewhat argillaceous.

Description of the Ilsemannite

The ilsemanite generally occurs as a cryptocrystalline or powdery incrustation on fluorite or altered granite. Frequently it appears as a halo, varying in thickness from a mere film up to several millimeters. It has also been noted as an impregnation in the matrix.

The color ranges from azure to blackish-blue. The lighter shades may well be due to the presence of intimately mixed, light-colored impurities. The streak is a pale blue. No method of obtaining material sufficiently pure for hardness and specific gravity determinations has been devised at the mine laboratory. Possibly the lack of data on these properties in the literature is due to a similar difficulty having been experienced by other investigators.

The mineral is sparingly soluble in distilled water. The solubility is greatly increased by the presence of small amounts of acids or alkalies. Cases are on record where the waters issuing from some mines are colored blue due to dissolved ilsemannite. Although much water originates in that part of the mine where the mineral is most abundant, no coloration has been imparted to it.

Mention has been made of the impossibility of separating pure ilsemannite for experimental purposes. Samples chosen for their above-average quality have invariably assayed low in molybdenum. The following partial analyses of picked specimens illustrate this:

Sample No.	Mo	Fe	S
83	0.185% (0.610%)*		
84	0.153% (0.504%)	1.592%	0.490%
85	0.614% (2.025%)	7.662%	3.211%
94	0.087% (0.288%)	0.860%	0.701%

* Figures in parentheses are Mo calculated to ilsemannite. 83—ilsemannite-bearing granite; 84—ore incrusted with ilsemannite; 85—disintegrated fault matter; 94—ilsemannite-incrusted ore.

Associates

Associated with the ilsemannite are quartz, feldspar, fluorite, ochre, chlorite, pyrite, gypsum, and melanterite. The first three make up the greater part of the vein matter. Chlorite and ochre are locally abundant, while the others are rare. No sulphides, other than pyrite, have been noted.

Commonly the fluorite exhibits a banded structure parallel to the vein walls. Granite inclusions are often surrounded by concentric fluorite "shells." An unusual structural phase for this mineral may be observed where the fissures have not been completely filled. Here it tends to become reniform on a large and spectacular scale. Well defined cubic crystals are uncommon and always small.

Scattered disseminations account for the greater part of the pyrite content. Occasionally inclusions, usually of fluorite, are found, surrounded by concentric rings of the sulphide—the so-called "cockade ore" (1). Some classic examples of this type have been collected from the deposit.

It has been stated that melanterite, $FeSO_4 \cdot 7H_2O$, always accompanies ilsemannite. Here it is found as a powdery, greenish-yellow incrustation, having the usual astringent taste. It is not always apparent in hand specimens, its presence being masked by other minerals, particularly ilsemannite and ochre. In some cases the melanterite and ilsemannite are mixed so intimately that a dark green product results.

Acknowledgments

The writer is indebted to the Western Fluorspar Corporation for permission to publish the results of the above analyses. Thanks are also due Mr. M. P. Cloonan, mine superintendent, for information and suggestions.

REFERENCES

1. DANA, E. S., *A System of Mineralogy.*
2. SCHALLER, W. T., *Jour. Wash. Acad. Sci.*, **7,** July 19 (1917).
3. HESS, FRANK L., *U. S. Geol. Surv., Bull.* **750,** 1–16 (1925).
4. LINDGREN, WALDEMAR, *Mineral Deposits,* 4th ed., p. 170 and fig. 59.

At the May meeting of the Philadelphia Mineralogical Society, Dr. Lincoln Dryden of Bryn Mawr College addressed the Society on the subject "Heavy Minerals as Guides to Geologic History." At the June meeting Dr. A. L. Patterson of Bryn Mawr was the speaker, his topic being "W. H. Bragg and his Contributions to Crystallography."

The following officers were recently elected by the New Jersey Mineralogical Society: President, J. D'Agostino; Vice-Presidents, Dr. S. S. Cole and O. I. Lee; Treasurer, O. B. J. Fraser; Secretaries, G. R. Stilwell and H. Hageman; Librarian, Edna M. Hensel; Curator, James M. Dupont.

NEW MINERAL NAMES

Rankinite

C. E. TILLEY: Tricalcium disilicate (rankinite), a new mineral from Scawt Hill, Co. Antrim. *Mineral. Mag.*, **26**, 190–196 (1942).

NAME: For G. A. Rankin, formerly physical chemist at the Geophysical Laboratory, who, with E. S. Shepherd and F. E. Wright, studied the systems CaO-SiO_2 and CaO-Al_2O_3-SiO_2 and first found the compound.

CHEMICAL PROPERTIES: The composition is $Ca_3Si_2O_7$. Insufficient material was available for quantitative analysis, identification being based on optical properties and microchemical tests. Gelatinizes readily in weak HCl-H_2SO_4 solutions, precipitating abundant gypsum. Contains no Mg nor Al. Unaffected by prolonged heating at 1100°. Melts incongruently at 1475°.

OPTICAL PROPERTIES: Monoclinic, $\alpha=1.640$–1.641, $\beta=1.644$, $\gamma=1.650$, $2V_\gamma 64°$, positive; $b=\beta$, α: edge of $(001)=15°$. These data agree with those given by Gordon (*Am. Mineral.*, **8**, 110 (1923) on crystals from slag.

OCCURRENCE: Found in two associations at Scawt Hill, Ireland; (a) as rounded or irregular grains in melilite rocks, associated with larnite or wollastonite in melilite, and (b) at the contact of flint nodules in metasomatized limestone, as a narrow zone of crystals separating wollastonite and larnite. Artificial material is also described from blast-furnace slag and from limestone xenoliths in glass from a bottle factory.

MICHAEL FLEISCHER

Correction

On page 619, Table 1, line J, in the column on observed epsilon index, the value 1.695 is that of epsilon *prime* rather than epsilon.